
Synthetic History: Evaluating Visual Representations of the Past in Diffusion Models

Maria-Teresa De Rosa Palmi
University of Zurich
maria-teresa.derosa-palmi@uzh.ch

Eva Cetinić
University of Zurich
eva.cetinic@uzh.ch

Abstract

As Text-to-Image (TTI) diffusion models become increasingly influential in content creation, growing attention is being directed toward their societal and cultural implications. While prior research has primarily examined demographic and cultural biases, the ability of these models to accurately represent historical contexts remains largely underexplored. In this work, we present a systematic and reproducible methodology for evaluating how TTI systems depict different historical periods. For this purpose, we introduce the *HistVis dataset*, a curated collection of 30,000 synthetic images generated by three state-of-the-art diffusion models using carefully designed prompts depicting universal human activities across different historical periods. We evaluate generated imagery across three key aspects: (1) **Implicit Stylistic Associations**: examining default visual styles associated with specific eras; (2) **Historical Consistency**: identifying anachronisms such as modern artifacts in pre-modern contexts; and (3) **Demographic Representation**: comparing generated racial and gender distributions against historically plausible baselines. Our findings reveal systematic inaccuracies in historically themed generated imagery, as TTI models frequently stereotype past eras by incorporating unstated stylistic cues, introduce anachronisms, and fail to reflect plausible demographic patterns. By offering a scalable methodology and benchmark for assessing historical representation in generated imagery, this work provides an initial step toward building more historically accurate and culturally aligned TTI models.

1 Introduction

Text-to-image (TTI) models have become powerful tools for generating high-quality images from text, with applications in different domains such as art, education, and media [46, 28]. However, recent critical analyses of TTI models highlight various issues, most notably the reinforcement of demographic biases, particularly gender and racial stereotypes [7, 26, 53, 4]. In addition, studies increasingly focus on cultural biases, such as Western-centric defaults and limited global diversity in the depiction of objects and traditions [47, 38].

While these studies primarily focus on present-day representations, how TTI models depict the past remains a largely underexplored area. Historical representation is not merely a matter of factual accuracy; it also reflects cultural memory, collective identity, and understandings of societal change. Synthetic imagery presents well-documented risks, such as the amplification of biases and stereotypes, the overlooking marginalized narratives [35], or the spread of misinformation [13]. When these issues appear in historically themed generated content, they can distort public understanding of the past and undermine the integrity of cultural memory. Despite these risks, current evaluation efforts often overlook how such distortions emerge in visual depictions of history.

Existing approaches to evaluating historical accuracy in foundation models predominantly focus on identifiable landmarks [49], prominent historical figures [22], or faithful reproduction of archival

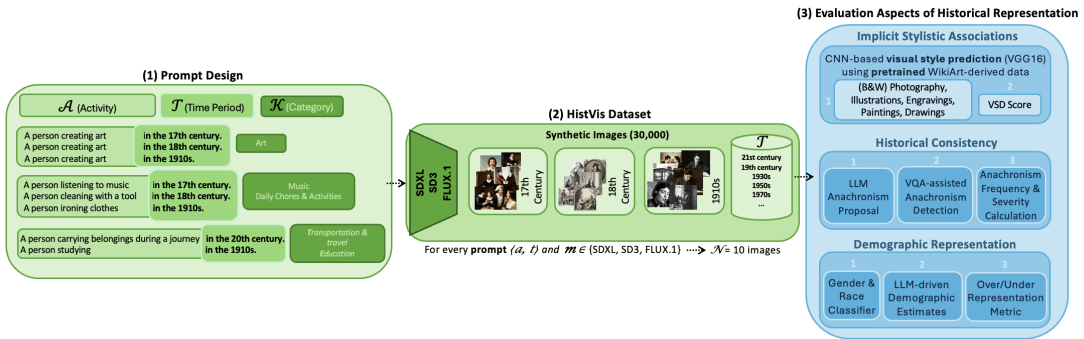


Figure 1: Overview of our methodology: (1) Prompt Design, (2) HistVis Dataset of synthetic images, and (3) Evaluation of stylistic bias, historical consistency, and demographic representation.

imagery [1]. However, such approaches overlook a more fundamental question: how do TTI models construct visual interpretations of the past? The widely publicized case of Google’s Gemini [45], which generated racially diverse Nazi soldiers, referred to as the “Black Nazi Problem” [19], highlighted the challenges of maintaining historical accuracy in AI-generated imagery and sparked debates on bias mitigation. Although AI bias is often discussed in terms of human representation, it also extends to the visual characteristics of generated images, such as the tendency of TTI models to associate certain historical periods with specific styles. Offert [32], for instance, describes the difficulty of generating color images of 1930s fascist parades without outputs defaulting to visual features of early Kodachrome or colorized black-and-white photography. Besides demographic and stylistic biases, TTI models often fail to preserve temporal coherence, resulting in anachronistic depictions of objects, settings, or behaviors, such as the appearance of smartphones in 18th-century scenes. Evaluating the historical reasoning of TTI models therefore requires a multifaceted approach that considers not only factual accuracy, but also implicit demographic assumptions, stylistic defaults, and the ability to produce temporally consistent representations.

To address these challenges, we introduce HistVis, a dataset of 30,000 synthetic images generated from 100 curated prompts covering 20 universal human activities (e.g., art, music) across five centuries (17th–21st) and five decades of the 20th century. We use three open-source diffusion models, Stable Diffusion XL (SDXL) [34], Stable Diffusion 3 (SD3) [15], and FLUX.1 Schnell¹, to generate images. As illustrated in Figure 1, we apply a reproducible evaluation methodology to the HistVis dataset to assess how TTI models depict historical contexts along three aspects: (1) Implicit Stylistic Associations, examining how models default to specific visual styles for different time periods; (2) Historical Consistency, identifying anachronisms such as modern artifacts in pre-modern contexts; and (3) Demographic Representation, assessing whether portrayals of race and gender align with historically plausible patterns. While HistVis is released in a fixed form, the proposed evaluation protocol remains reusable for analyzing the historical understanding of other TTI models.

To the best of our knowledge, this is the first systematic evaluation of how diffusion models represent historical contexts, providing a foundation for assessing representational fidelity and the underlying biases that shape the portrayal of the past in generated imagery.

2 Related Work

TTI models have rapidly evolved from technical innovations into widely adopted tools with broad societal impact. As Cetinić [5] argues, these models function as “cultural snapshots”, encoding not only the culturally specific associations present in their training data but also the culturally contingent decisions made during model development. Consequently, they should be studied not just as tools but as artifacts that reveal tensions between neutrality, memorization and the politics of representation.

One significant dimension through which these tensions become evident is in demographic bias, particularly along gender and racial lines, which remains among the most extensively studied aspects of cultural encoding in TTI models. Studies consistently show that these biases manifest as stereotypical associations, such as overrepresenting women in caregiving roles and men in technical

¹<https://huggingface.co/black-forest-labs/FLUX.1-schnell>

professions, thereby reinforcing existing social hierarchies [40, 17]. Methodologically, these patterns have been identified through comparisons with real-world benchmarks such as labor statistics [26, 4, 27], embedding-based bias metrics [29], and classifier-based audits using models like BLIP-2 to evaluate responses to neutral occupational prompts [9]. Recent work further reveals that these biases not only affect the portrayal of gender but also associated objects and image layouts [51].

Beyond demographic biases, TTI models struggle with cultural representations, often reinforcing dominant narratives while failing to capture regional nuances. Minor prompt modifications, such as replacing a Latin character with a Greek or Arabic homograph, can dramatically shift outputs toward stereotypical depictions [42]. Neutral prompts also tend to produce Western-centric imagery, reflecting a lack of region-specific authenticity [47]. Benchmarks like CUBE [38] and UCOGC [52] show that even culturally specific prompts (e.g., India’s *gopuram*) often fail to yield accurate representations. Moreover, omitting country names can skew outputs toward U.S. or Indian-centric outputs, highlighting the need for globally aware and context-sensitive TTI systems [3].

While demographic and cultural biases in TTI models have received considerable attention, historical representation remains a relatively underexplored dimension. In one of the few works to address the concept of history in TTI models, Offert discusses their stylistic biases and their tendency to produce visually reductive portrayals of the past [32]. Related studies on AI-generated “promptography” show that models may produce convincing yet erroneous outputs that mimic historical artifacts, thereby revealing the constructed nature of these depictions [30]. Beyond image generation, hallucinated narratives in conversational or museum-based AI systems further shape public perceptions, amplifying the risk of historical distortion [50]. Taken together, these findings indicate that while generative AI is capable of reconstructing historical imagery, it frequently does so in a selective, imprecise, and oversimplified manner.

Although some recent work started to address history-related tasks, these efforts tend to focus on recognition and factual alignment. For example, CENTURY [1] investigates how accurately multimodal models describe sensitive historical photographs, while HEIM [22] and the Google Landmarks Dataset v2 [49] evaluate recognition of historical figures and landmarks. However, these existing benchmarks focus on factual correctness and identification rather than probing how models contextualize representations of the past.

Despite growing recognition of the socio-cultural implications of TTI systems, their historical grounding remains largely underexplored. Our work introduces a systematic framework for evaluating historical representation in generated imagery, positioning historical depiction as a key dimension of cultural reasoning in generative models.

3 The HistVis Dataset

As part of our evaluation, we introduce *HistVis*, a dataset comprising synthetic images generated from prompts describing historically situated universal human activities. Each prompt follows the template “A person [activity] in the [time period].” To ensure comprehensive representation, we define 100 distinct activities $\mathcal{A} = \{a_1, \dots, a_{100}\}$, each belonging to one of 20 diverse categories $\mathcal{K} = \{k_1, \dots, k_{20}\}$ covering domains such as art, religion, agriculture, work, daily chores, and others, as detailed in Appendix A. These prompts emphasize timeless practices rather than period-specific objects or situations, allowing the evaluation to focus on how models represent activities across different periods. For example, prompts like “A person listening to music” or “A person traveling” describe universal behaviors that transcend historical context.

Each activity is paired with 10 historical time periods $\mathcal{T} = \{t_1, \dots, t_{10}\}$, spanning five centuries (17th–21st) and five decades of the 20th-century (1910, 1930, 1950, 1970, 1990). For example, the prompt “A person listening to music” can be adapted by adding “in the 17th century” or “in the 1910s,” to explore how the same universal activity is depicted across various time periods. The selected time periods balance broad historical coverage with finer temporal resolution: centuries capture long-term cultural trends, while 20th-century decades reveal more nuanced societal shifts. Although these choices serve our goals, alternative periods could highlight different aspects of historical representation.

For each combination of activity and time period, represented as pairs $\langle a, t \rangle$, where $a \in \mathcal{A}$ and $t \in \mathcal{T}$, we generate images using three TTI models: SDXL, SD3, and FLUX.1 using Nvidia A100 GPU

with 24 CPU cores, 64GB RAM, and Python 3.12.1. These models were selected because they are state-of-the-art open-source diffusion models and allow for a comparison between two versions of the same system. For each model $m \in \{\text{SDXL}, \text{SD3}, \text{FLUX.1}\}$, we generate $N = 10$ outputs per $\langle a, t \rangle$, resulting in a total of 30,000 images. Both the dataset², including all associated metadata, and our reproducible evaluation scripts³ are publicly available under cc by-nc 4.0 license.

4 Implicit Stylistic Associations

The first aspect of our evaluation examines whether TTI models default to stylistic cues for historical periods, even when such features are not specified in the prompt. Leveraging the structure of the HistVis dataset, where the activity remains fixed and only the time period varies, we introduce a methodology to quantify the strength and consistency of these associations across models and periods, enabling systematic analysis of a phenomenon previously described only qualitatively [32].



Figure 2: Examples of generated images reflecting different stylistic biases when a specific time period is added to the prompt “A person expressing joy after achieving a goal”.

4.1 Experimental Setup

To systematically analyze these implicit associations, we use a trained CNN-based model to predict the visual styles of generated images. The model is trained on a WikiArt-derived dataset⁴ and fine-tuned to distinguish five stylistic categories: drawings, engravings, illustrations, paintings and photography. These categories were selected because they represent significantly distinct stylistic modes that emerged consistently in our initial qualitative analysis of historically situated generated images. Although not exhaustive, this selection provides a structured foundation for identifying patterns of stylistic bias in generated images.

We fine-tune a VGG16 [41] pre-trained on ImageNet [21], using a WikiArt-derived dataset with 1,500 images per stylistic category. CNN-based classifiers trained on artwork datasets effectively capture both low- and high-level stylistic features [44, 6], making them a simple and well-suited approach for detecting stylistic patterns in generated images. Since WikiArt does not distinguish between monochrome and color photography, we refine predictions using the colorfulness metric proposed by Hasler and Suesstrunk [18] to quantify color distribution and intensity. Within the photography category, images with a colorfulness score below 10, including both b&w and sepia tones, are labeled as monochrome. For our style classifier, we explore different fine-tuning strategies and achieve the best classification accuracy of 0.86 when retraining only the last layer, as detailed in Appendix B. Once trained, the classifier is applied to the generated images in our HistVis dataset to predict their closest stylistic category, revealing model-specific tendencies in historical representation.

4.2 Visual Style Dominance (VSD) Score

We define the *Visual Style Dominance (VSD)* score to measure the extent to which the outputs of a TTI model for a given historical period converge on a single visual style. For a model m and time period t , the score is defined as:

$$\text{VSD}(m, t) = \max_s P_m(s | t), \tag{1}$$

²Hugging Face Repository

³GitHub Repository

⁴<https://www.wikiart.org/>

where $P_m(s | t)$ is the proportion of images generated by model m for period t that are predicted as style s . Higher VSD values indicate stronger associations between historical periods and specific visual styles, while lower values suggest weaker convergence.

Table 1: VSD scores and dominant visual styles by model and historical period. The final columns indicate changes in SDXL after prompt engineering.

Period	FLUX.1		SD3		SDXL		SDXL → Mitigated	
	Score	Visual Style	Score	Visual Style	Score	Visual Style	Score	Visual Style
17th c.	0.90	painting	0.88	painting	0.95	engraving	0.85	engraving ↓↔
18th c.	0.86	painting	0.81	painting	0.91	engraving	0.82	engraving ↓↔
19th c.	0.60	painting	0.66	painting	0.63	engraving	0.53	engraving ↓↔
20th c.	0.85	photog.	0.68	photog.	0.37	illustr.	0.80	illustr. ↑↔
21st c.	0.86	photog.	0.96	photog.	0.85	illustr.	0.92	illustr. ↑↔
1910s	0.77	monochrome	0.84	monochrome	0.71	monochrome	0.80	painting ↑↔
1930s	0.79	monochrome	0.81	monochrome	0.75	monochrome	0.53	painting ↓↔
1950s	0.51	monochrome	0.55	monochrome	0.68	monochrome	0.84	illustr. ↑↔
1970s	0.93	photog.	0.87	photog.	0.35	photog.	0.72	illustr. ↑↔
1990s	0.97	photog.	0.98	photog.	0.52	illustr.	0.58	illustr. ↑↔

Legend: ↑↓: Score increase/decrease; ↔: Unchanged; ⇔: Style changed.

Results Table 1 presents VSD scores for each model across the historical periods. For the 17th and 18th centuries, SDXL shows high VSD scores for engravings, while SD3 and FLUX.1 favor painting aesthetics. In the 20th and 21st centuries, SD3 and FLUX.1 shift toward photography, while SDXL exhibits more stylistic variation, with a strong preference for illustrations. All three models show dominance for monochrome outputs in earlier decades of the 20th century such as the 1910s, 1930s, and 1950s. Figure 2 provides examples illustrating these stylistic biases. To assess mitigation potential, we experimented with prompt engineering, a strategy for bias reduction in both text and image generation [10, 14], by explicitly requesting photorealism and discouraging monochrome outputs through the negative prompt. As shown in the final columns of Table 1, dominance scores decrease in some periods (e.g., 17th–18th centuries), and dominant styles occasionally shift (e.g., from monochrome to painting). However, these changes rarely achieve the intended goal of photorealism, suggesting that stylistic defaults are persistent and not easily overridden at the prompt level. A detailed overview of the stylistic distributions across models and periods is provided in Appendix B.

5 Historical Consistency

The second aspect of historical representation that we evaluate is historical consistency. This involves assessing whether TTI models introduce *anachronisms*, e.g. modern artifacts in the depiction of pre-modern contexts. Inspired by the open-set bias detection strategies proposed by D’Incà et al. [12] and Chinchure et al. [8], which identify biases without predefined categories and focus on cultural issues (e.g., gender stereotypes, brand associations), we apply a similar approach to target anachronisms and propose an automated detection methodology which we validate through human judgment.

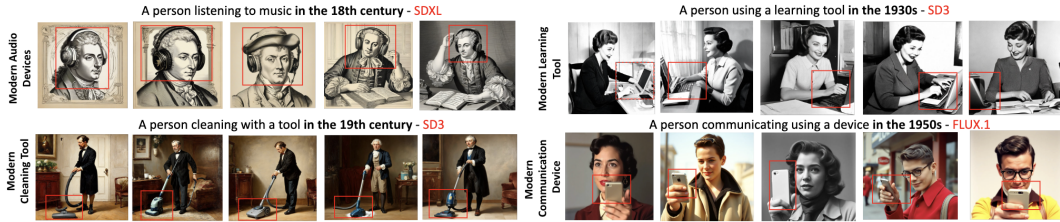


Figure 3: Examples of generated images with anachronisms identified by our two-stage method: headphones in the 18th, vacuum cleaner in the 19th-century, laptop in 1930s and smartphone in 1950s.

5.1 Anachronism Detection

Our anachronism detection method is applied to the same structured prompts defined in *HistVis*, where each prompt is a combination of a human activity and a historical time period, denoted as $\langle a, t \rangle$. The detection pipeline consists of two stages: (i) LLM-guided Anachronism Proposal and (ii) VQA-based Anachronism Detection. For both stages, we use GPT-4o as the underlying foundational model due to its state-of-the-art performance across a variety of tasks [25, 24, 23], as well as its strong zero-shot visual recognition capabilities [19].

Given a prompt $\langle a, t \rangle$, GPT-4o is used to generate a set of potential anachronistic elements $\mathcal{Z}_{a,t} = \{z_1, \dots, z_k\}$ in the historical context defined by t . For each proposed anachronism z_i , it also produces a corresponding binary yes/no question q_i designed to identify whether the anachronism appears in the generated image. For example, given the prompt “A person listening to music in the 18th century,” the LLM might return the anachronism “modern audio devices” along with the identification question “Is the person using modern audio devices, such as headphones or smartphones that didn’t exist in the 18th century? Answer with ‘yes’ or ‘no’.”

Given the generated image $I_{a,t}^m$ and its associated set of anachronism identification questions $\mathcal{Q}_{a,t} = \{(z_i, q_i)\}$, we use GPT-4o’s vision capabilities in a VQA setup to answer each question q_i with a binary yes/no response, indicating whether the corresponding anachronistic element z_i is visually present in the image. This method enables flexible, open-ended detection of historically implausible elements in generated outputs, without relying on predefined object lists.

Anachronism Assessment Metrics To systematically evaluate anachronisms in generated images, we first normalize minor lexical variations in the phrasing of proposed anachronisms introduced by the LLM. For instance, a model may refer to the same object as “modern audio device” in one case and “digital audio device” in another. To avoid double-counting these identical references, we apply *fuzzy matching* [37] to treat them as the same entry. Importantly, this normalization only addresses surface-level naming inconsistencies and does not involve semantic grouping of distinct concepts.

For each time period $t \in \mathcal{T}$ and each TTI model $m \in \{\text{SDXL}, \text{SD3}, \text{FLUX.1}\}$, we compute two metrics for each anachronistic element z_i proposed by the LLM. *Frequency* is defined as the proportion of generated images (for the given time period and model) in which z_i is detected, and *Severity* as the consistency with which the model introduces z_i once it is proposed by the LLM. Formally, we define:

$$\text{Frequency}(z_i, t, m) = \frac{n_{z_i}^{\text{detected}}}{N_t^m}, \quad \text{Severity}(z_i) = \frac{n_{z_i}^{\text{detected}}}{n_{z_i}^{\text{proposed}}}, \quad (2)$$

where N_t^m is the total number of images generated by model m for time period t , $n_{z_i}^{\text{detected}}$ is the number of images in which z_i is detected, and $n_{z_i}^{\text{proposed}}$ is the number of prompts in which the LLM proposed z_i as a plausible anachronism. For example, if “modern phone equipment” is detected in 10 out of 1,000 images for the 18th century, its frequency is 1%, and if it is proposed in exactly 10 instances and appears in all 10, then its severity is 1.0.

5.2 Anachronism Frequency & Severity Scores

Figure 4 plots the top 15 anachronistic elements per model, ranked independently by *frequency* and *severity*, aggregated across all centuries. Each data point corresponds to an element proposed by the LLM and confirmed via VQA, with fuzzy matching applied to unify lexical variations. For example, *clothing* appears in about 2-5% of all anachronistic images, making it the most frequent item overall, yet it shows relatively low severity, indicating a scattered but recurring misrepresentation. By contrast, items like *audio devices* and *ironing equipment* occur less often but with higher severity: when these elements are proposed by the LLM as plausible anachronisms for a given prompt, they are almost always identified in the corresponding generated images. This behavior suggests that models often rely more on the prompt’s conceptual cues (e.g., “listening to music”) than on the intended historical context, revealing a structural lapse in historical conditioning. Furthermore, SD3 appears most prone to anachronisms, with 20% of its 19th-century and 25% of its 1930s images flagged, followed by FLUX.1 and SDXL, revealing varying model tendencies. Examples of high-severity anachronisms are shown in Figure 3, with detailed breakdowns in Appendix E.

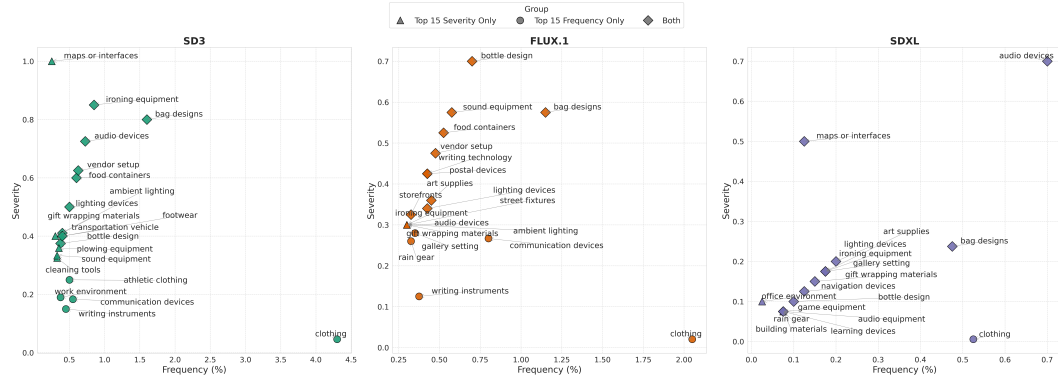


Figure 4: Top 15 anachronistic elements per model, ranked by frequency (x-axis) and severity (y-axis). Circles indicate elements in the top 15 by frequency, triangles by severity, and diamonds by both.

User Study. To evaluate the alignment between our proposed anachronism detection method and human judgment, we conducted an anonymous user study on a public crowdsourcing platform with no geographical restrictions. Since SD3 had the highest anachronism rate, we randomly sampled 200 images per decade and century from that model, yielding 1,800 images overall. Each image was evaluated by three participants, producing 5,400 annotations. To ensure data quality, we only retained responses from users who correctly answered predefined control questions, indicating task understanding. For the final analysis, we included only images with exactly three responses from these reliable users, resulting in 2,040 responses from 234 users. A majority vote served as the human baseline. Our proposed approach agreed with the majority human judgment on 72% of the images, indicating substantial alignment with human baseline well above chance level. Appendix G provides additional details on the interface, instructions, and data collection.

6 Demographic Representation

The third aspect we evaluate is demographic representation, using the HistVis dataset to analyze gender and racial portrayals in AI-generated historically situated images. We assess whether the models reflect historically plausible demographics instead of modern expectations, as an indication of their temporal understanding. However, establishing "historical plausibility" is extremely challenging, given the lack of precise records, regional variability, and the complex interplay between social roles, race, and gender across different time periods. To approximate expectations, we use LLM-based estimates that synthesize contextual knowledge for each activity and time period. While this method offers a scalable baseline, it remains a coarse approximation for historical accuracy and inherits the limitations and biases of the language model itself.

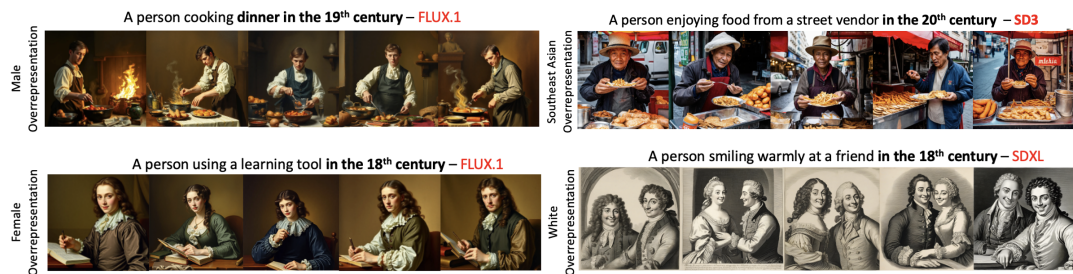


Figure 5: Examples of generated images illustrating demographic overrepresentation across models, time periods, and activities.

6.1 Methodology

To evaluate demographic representation in historically conditioned TTI-generated images, we developed a pipeline that compares generated demographic attributes to historically plausible expectations. This pipeline comprises three steps: (1) extracting demographic attributes from generated images

using an automated face classifier, (2) estimating historical demographics with an LLM that synthesizes contextual knowledge for each activity–time pair, and (3) applying a metric-based comparison to quantify the extent of demographic under- or overrepresentation.

Demographic Extraction from Generated Images. We use the FairFace classifier [20], a ResNet34-based model trained on 108,501 facial images with balanced demographic attributes, to detect gender (male, female) and race (White, Black, Indian, East Asian, Southeast Asian, Middle Eastern, Latino) in generated images, including those with multiple faces. For each image $I_{(a,t)}$ corresponding to an activity, period pair $\langle a, t \rangle$, the classifier returns predictions $\{(g_j, r_j, c_j^{\text{gender}}, c_j^{\text{race}})\}_{j=1}^n$, where g_j and r_j denote the gender and race of the j th face, and $c_j^{\text{gender}}, c_j^{\text{race}} \in [0, 1]$ are the associated confidence scores. Predictions with confidence below 0.7 in either attribute are discarded to minimize misclassification risk. We compute demographic proportions by normalizing valid predictions over all detected faces in each image, then average across the N images generated for each pair $\langle a, t \rangle$, resulting in the distributions $P_{\text{gender}}^m(a, t)$ and $P_{\text{race}}^m(a, t)$.

To validate prediction reliability, we employ the DeepFace classifier [39], an ensemble of facial analysis models including VGG-Face [33], FaceNet [36], DeepFace [43], and ArcFace [11]. Using 5,000 randomly sampled images (500 per time period/model pair), we find strong inter-model agreement of 95.9% for gender ($\kappa = 0.93$) and 90.8% for race ($\kappa = 0.83$), where κ denotes Cohen’s kappa coefficient measuring inter-rater reliability.

Estimating Historical Demographic Baselines. To assess whether generated demographic distributions align with historically plausible expectations, we use GPT-4o to estimate the expected breakdown for each activity–period pair $\langle a, t \rangle$. For each case, we query it with: “Given the [activity] and the [historical period], estimate the plausible demographic breakdown (in percentages) for gender and race.” It then returns percentage-based estimates $\hat{P}_{\text{gender}}^{\text{llm}}(a, t)$ and $\hat{P}_{\text{race}}^{\text{llm}}(a, t)$.

These values are not treated as definitive ground truth, but rather as approximations that help assess whether TTI outputs diverge significantly from LLM-derived, historically grounded demographic expectations. More details on the LLM input formatting are provided in Appendix H.

Under & Overrepresentation Metric. We propose two metrics, *underrepresentation* and *overrepresentation*, to quantify how closely TTI-generated images align with historically plausible demographic expectations. Inspired by fairness metrics in ML that quantify deviations from reference distribution [48, 17, 4], our approach adapts these to the historical domain using LLM-derived estimates rather than population statistics. For each activity–period pair $\langle a, t \rangle$ and demographic category $d \in \{\text{male, female, White, Black, Middle Eastern, Indian, Southeast Asian, East Asian}\}$, we compute both metrics. Formally, let P_d^{model} denote the proportion of demographic group d observed in the generated images, and \hat{P}_d^{llm} the corresponding estimate provided by the LLM. We define:

$$\text{Under}_d = \mathbb{I}\{P_d^{\text{model}} < \hat{P}_d^{\text{llm}}\} \cdot [\hat{P}_d^{\text{llm}} - P_d^{\text{model}}], \quad (3)$$

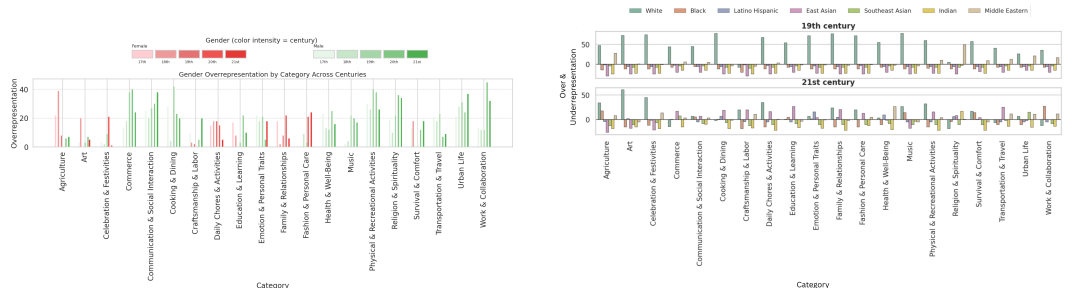
$$\text{Over}_d = \mathbb{I}\{P_d^{\text{model}} > \hat{P}_d^{\text{llm}}\} \cdot [P_d^{\text{model}} - \hat{P}_d^{\text{llm}}] \quad (4)$$

These two metrics measure the absolute deviation in cases where the TTI model either underrepresents or overrepresents a demographic group relative to the LLM-derived historically plausible baseline. We compute these values for each prompt and then aggregate them at the domain category level (e.g., education, religion, arts) to identify systematic demographic disparities across broader cultural contexts. Although our focus is on neutral activities in the *HistVis* dataset, this pipeline can also flag cases where generated outputs deviate from historical norms.

6.2 Demographic Alignment Evaluation

When comparing GPT-4o-derived demographic baselines with face classifier predictions across TTI models, we find frequent divergences from historically plausible patterns, with variation depending on the model. As shown in Figure 6a, FLUX.1 tends to overrepresent male figures, even in categories like “cooking & dining,” where GPT-4o estimates a predominantly female presence until the 20th century. This male bias persists across centuries, including in “work & collaboration,” which GPT-4o anticipates becoming gender-balanced by the 21st century. Conversely, “education & learning” skews

female in the 17th–18th centuries, although GPT-4o indicates male majorities during that period. White individuals are generally overrepresented across models, though this trend diminishes by the 21st century, aligning closer to historical expectations. However, specific categories (e.g., "religion & spirituality," "agriculture") show pronounced spikes in non-White representations, as illustrated in Figure 6b for FLUX.1. Similar trends are visible across other models and time periods, suggesting that these distributions may reflect correlations in the training data rather than historically grounded depictions. Additional figures with representation scores across all models, time periods, and activity categories are provided in Appendix H.3.



(a) Gender overrepresentation across the 17th–21st centuries. (b) Racial under- and overrepresentation in the 19th and 21st century.

Figure 6: Gender and racial over-/underrepresentation in FLUX.1 outputs across different centuries and activities, measured as absolute deviations from GPT-4o demographic baselines.

7 Discussion and Limitations

Our analysis reveals that TTI models rely on limited stylistic encodings rather than nuanced understandings of historical periods. Each era is strongly tied to a specific visual style, resulting in one-dimensional portrayals of history. Notably, photorealistic depictions of people appear only from the 20th century onward, with only rare exceptions in FLUX.1 and SD3, suggesting that models reinforce learned associations rather than flexibly adapting to historical contexts, perpetuating the notion that realism is a modern trait. In addition, frequent anachronisms suggest that historical periods are not cleanly separated in the latent spaces of these models, since modern artifacts often emerge in pre-modern settings, undermining the reliability of TTI systems in education and cultural heritage contexts. Finally, demographic representations underscore a lack of historical awareness: some outputs depict historically underrepresented groups at implausibly high rates, whereas others reproduce contemporary biases. This inconsistency highlights a deeper challenge in bias mitigation: correcting past exclusions risks distorting historical accuracy, yet faithfully reproducing historical inequalities may reinforce exclusionary narratives. Striking a balance between these goals remains therefore an open challenge.

While our study offers the first systematic evaluation of historical representation in TTI models, it is constrained by several important limitations. First, our analysis of stylistic defaults relies on broad categories and does not capture finer distinctions. Second, while we selected a range of centuries and decades to capture broad trends and subtler shifts, these choices were somewhat arbitrary; alternative periods might yield different insights. Third, we based our prompts on universal activities, which could omit details relevant to specific historical contexts. Fourth, while our use of LLMs for demographic estimation and anachronism detection demonstrates promising initial results, we remain mindful of the challenges inherent in historical analysis, the potential biases highlighted in prior research [16, 31], and the fact that LLMs cannot replace the depth or reliability of expert historical knowledge. We are also aware that our baselines are significantly simplified, averaging demographic expectations across time and activity and omitting other factors. Similarly, the use of face classifiers further simplifies social complexities, reducing gender and race to discrete categories. Finally, while our anachronism pipeline was validated with a user study, judgments may vary due to differences in historical expertise and subjective interpretation. However, our approach establishes a strong basis for systematically evaluating historical aspects of TTI models, and its flexibility allows application to future models for continuous improvement.

References

- [1] Canfer Akbulut, Kevin Robinson, Maribeth Rauh, Isabela Albuquerque, Olivia Wiles, Laura Weidinger, Verena Rieser, Yana Hasson, Nahema Marchal, Iason Gabriel, William Isaac, and Lisa Anne Hendricks. CENTURY: A framework and dataset for evaluating historical contextualisation of sensitive images. In *Proceedings of the International Conference on Learning Representations (ICLR)*. OpenReview, 2025. URL <https://openreview.net/forum?id=1KLBvrYz3V>. Published at ICLR 2025.
- [2] Mohammadreza Armandpour, Ali Sadeghian, Huangjie Zheng, Amir Sadeghian, and Mingyuan Zhou. Re-imagine the negative prompt algorithm: Transform 2d diffusion into 3d, alleviate janus problem and beyond. *arXiv preprint arXiv:2304.04968*, 2023.
- [3] Abhipsa Basu, R Venkatesh Babu, and Danish Pruthi. Inspecting the geographical representativeness of images from text-to-image models. In *Proceedings of the IEEE/CVF International Conference on Computer Vision*, pages 5136–5147, 2023.
- [4] Federico Bianchi, Pratyusha Kalluri, Esin Durmus, Faisal Ladhak, Myra Cheng, Debora Nozza, Tatsunori Hashimoto, Dan Jurafsky, James Zou, and Aylin Caliskan. Easily accessible text-to-image generation amplifies demographic stereotypes at large scale. In *Proceedings of the 2023 ACM Conference on Fairness, Accountability, and Transparency*, pages 1493–1504, 2023.
- [5] Eva Cetinic. The myth of culturally agnostic ai models. *arXiv preprint arXiv:2211.15271*, 2022.
- [6] Eva Cetinic, Tomislav Lipic, and Sonja Grgic. Fine-tuning convolutional neural networks for fine art classification. *Expert Systems with Applications*, 114:107–118, 2018.
- [7] Aadi Chauhan, Taran Anand, Tanisha Jauhari, Arjav Shah, Rudransh Singh, Arjun Rajaram, and Rithvik Vanga. Identifying race and gender bias in stable diffusion ai image generation. In *2024 IEEE 3rd International Conference on AI in Cybersecurity (ICAIC)*, pages 1–6. IEEE, 2024.
- [8] Aditya Chinchure, Pushkar Shukla, Gaurav Bhatt, Kiri Salij, Kartik Hosanagar, Leonid Sigal, and Matthew Turk. Tibet: Identifying and evaluating biases in text-to-image generative models. In *European Conference on Computer Vision*, pages 429–446. Springer, 2024.
- [9] Jaemin Cho, Abhay Zala, and Mohit Bansal. Dall-eval: Probing the reasoning skills and social biases of text-to-image generation models. In *Proceedings of the IEEE/CVF International Conference on Computer Vision*, pages 3043–3054, 2023.
- [10] Colton Clemmer, Junhua Ding, and Yunhe Feng. Precisedebias: An automatic prompt engineering approach for generative ai to mitigate image demographic biases. In *Proceedings of the IEEE/CVF Winter Conference on Applications of Computer Vision*, pages 8596–8605, 2024.
- [11] Jiankang Deng, Jia Guo, Niannan Xue, and Stefanos Zafeiriou. Arcface: Additive angular margin loss for deep face recognition. In *Proceedings of the IEEE/CVF conference on computer vision and pattern recognition*, pages 4690–4699, 2019.
- [12] Moreno D’Inca, Elia Peruzzo, Massimiliano Mancini, Dejie Xu, Vidit Goel, Xingqian Xu, Zhangyang Wang, Humphrey Shi, and Nicu Sebe. Openbias: Open-set bias detection in text-to-image generative models. In *Proceedings of the IEEE/CVF Conference on Computer Vision and Pattern Recognition*, pages 12225–12235, 2024.
- [13] Nicholas Dufour, Arkanath Pathak, Pouya Samangouei, Nikki Hariri, Shashi Deshetti, Andrew Dudfield, Christopher Guess, Pablo Hernández Escayola, Bobby Tran, Mevan Babakar, et al. Ammeba: A large-scale survey and dataset of media-based misinformation in-the-wild. *arXiv preprint arXiv:2405.11697*, 2024.
- [14] Satyam Dwivedi, Sanjukta Ghosh, and Shivam Dwivedi. Breaking the bias: Gender fairness in llms using prompt engineering and in-context learning. *Rupkatha Journal on Interdisciplinary Studies in Humanities*, 15(4), 2023.
- [15] Patrick Esser, Sumith Kulal, Andreas Blattmann, Rahim Entezari, Jonas Müller, Harry Saini, Yam Levi, Dominik Lorenz, Axel Sauer, Frederic Boesel, et al. Scaling rectified flow transformers for high-resolution image synthesis. In *Forty-first international conference on machine learning*, 2024.

- [16] Isabel O Gallegos, Ryan A Rossi, Joe Barrow, Md Mehrab Tanjim, Sungchul Kim, Franck Dernoncourt, Tong Yu, Ruiyi Zhang, and Nesreen K Ahmed. Bias and fairness in large language models: A survey. *Computational Linguistics*, 50(3):1097–1179, 2024.
- [17] Siobhan Mackenzie Hall, Fernanda Gonçalves Abrantes, Hanwen Zhu, Grace Sodunke, Aleksandar Shtedritski, and Hannah Rose Kirk. Visogender: A dataset for benchmarking gender bias in image-text pronoun resolution. *Advances in Neural Information Processing Systems*, 36:63687–63723, 2023.
- [18] David Hasler and Sabine E Suesstrunk. Measuring colorfulness in natural images. In *Human vision and electronic imaging VIII*, volume 5007, pages 87–95. SPIE, 2003.
- [19] Tonja Jacobi and Matthew Sag. We are the ai problem. *Emory LJ Online*, 74:1, 2024.
- [20] Kimmo Karkkainen and Jungseock Joo. Fairface: Face attribute dataset for balanced race, gender, and age for bias measurement and mitigation. In *Proceedings of the IEEE/CVF winter conference on applications of computer vision*, pages 1548–1558, 2021.
- [21] Alex Krizhevsky, Ilya Sutskever, and Geoffrey E Hinton. Imagenet classification with deep convolutional neural networks. *Advances in neural information processing systems*, 25, 2012.
- [22] Tony Lee, Michihiro Yasunaga, Chenlin Meng, Yifan Mai, Joon Sung Park, Agrim Gupta, Yunzhi Zhang, Deepak Narayanan, Hannah Teufel, Marco Bellagente, et al. Holistic evaluation of text-to-image models. *Advances in Neural Information Processing Systems*, 36:69981–70011, 2023.
- [23] Xuechen Li, Tianyi Zhang, Yann Dubois, Rohan Taori, Ishaan Gulrajani, Carlos Guestrin, Percy Liang, and Tatsunori B Hashimoto. AlpacaEval: An automatic evaluator of instruction-following models, 2023.
- [24] Zheng Lian, Licai Sun, Haiyang Sun, Kang Chen, Zhuofan Wen, Hao Gu, Bin Liu, and Jianhua Tao. Gpt-4v with emotion: A zero-shot benchmark for generalized emotion recognition. *Information Fusion*, 108:102367, 2024.
- [25] Pan Lu, Hritik Bansal, Tony Xia, Jiacheng Liu, Chunyuan Li, Hannaneh Hajishirzi, Hao Cheng, Kai-Wei Chang, Michel Galley, and Jianfeng Gao. Mathvista: Evaluating mathematical reasoning of foundation models in visual contexts. *arXiv preprint arXiv:2310.02255*, 2023.
- [26] Sasha Luccioni, Christopher Akiki, Margaret Mitchell, and Yacine Jernite. Stable bias: Evaluating societal representations in diffusion models. *Advances in Neural Information Processing Systems*, 36, 2024.
- [27] Hanjun Luo, Haoyu Huang, Ziyi Deng, Xuecheng Liu, Ruizhe Chen, and ZuoZhu Liu. Bigbench: A unified benchmark for social bias in text-to-image generative models based on multi-modal llm. *arXiv preprint arXiv:2407.15240*, 2024.
- [28] Adyasha Maharana, Darryl Hannan, and Mohit Bansal. Storydall-e: Adapting pretrained text-to-image transformers for story continuation. In *European Conference on Computer Vision*, pages 70–87. Springer, 2022.
- [29] Abhishek Mandal, Susan Leavy, and Suzanne Little. Measuring bias in multimodal models: Multimodal composite association score. In *International Workshop on Algorithmic Bias in Search and Recommendation*, pages 17–30. Springer, 2023.
- [30] Juan Martín Prada. Ai-based generative image production systems in the artistic problematisation of the past: the thematisation of memory and temporality in "ai art". *AI & SOCIETY*, pages 1–12, 2025.
- [31] Roberto Navigli, Simone Conia, and Björn Ross. Biases in large language models: origins, inventory, and discussion. *ACM Journal of Data and Information Quality*, 15(2):1–21, 2023.
- [32] Fabian Offert. On the concept of history (in foundation models). 2023.

- [33] Omkar Parkhi, Andrea Vedaldi, and Andrew Zisserman. Deep face recognition. In *BMVC 2015-Proceedings of the British Machine Vision Conference 2015*. British Machine Vision Association, 2015.
- [34] Dustin Podell, Zion English, Kyle Lacey, Andreas Blattmann, Tim Dockhorn, Jonas Müller, Joe Penna, and Robin Rombach. Sdxl: Improving latent diffusion models for high-resolution image synthesis. *arXiv preprint arXiv:2307.01952*, 2023.
- [35] Habiba Sarhan and Simon Hegelich. Understanding and evaluating harms of ai-generated image captions in political images. *Frontiers in Political Science*, 5:1245684, 2023.
- [36] Florian Schroff, Dmitry Kalenichenko, and James Philbin. Facenet: A unified embedding for face recognition and clustering. In *Proceedings of the IEEE conference on computer vision and pattern recognition*, pages 815–823, 2015.
- [37] SeatGeek. Fuzzywuzzy: Fuzzy string matching in python. <https://github.com/seatgeek/fuzzywuzzy>, 2011.
- [38] Nithish Kannan Senthilkumar, Arif Ahmad, Marco Andreetto, Vinodkumar Prabhakaran, Utsav Prabhu, Adji Bousso Dieng, Pushpak Bhattacharyya, and Shachi Dave. Beyond aesthetics: Cultural competence in text-to-image models. *Advances in Neural Information Processing Systems*, 37:13716–13747, 2024.
- [39] Sefik Ilkin Serengil and Alper Ozpinar. Lightface: A hybrid deep face recognition framework. In *2020 innovations in intelligent systems and applications conference (ASYU)*, pages 1–5. IEEE, 2020.
- [40] Preethi Seshadri, Sameer Singh, and Yanai Elazar. The bias amplification paradox in text-to-image generation. *arXiv preprint arXiv:2308.00755*, 2023.
- [41] Karen Simonyan and Andrew Zisserman. Very deep convolutional networks for large-scale image recognition. *arXiv preprint arXiv:1409.1556*, 2014.
- [42] Lukas Struppek, Dom Hintersdorf, Felix Friedrich, Patrick Schramowski, Kristian Kersting, et al. Exploiting cultural biases via homoglyphs in text-to-image synthesis. *Journal of Artificial Intelligence Research*, 78:1017–1068, 2023.
- [43] Yaniv Taigman, Ming Yang, Marc’ Aurelio Ranzato, and Lior Wolf. Deepface: Closing the gap to human-level performance in face verification. In *Proceedings of the IEEE conference on computer vision and pattern recognition*, pages 1701–1708, 2014.
- [44] Wei Ren Tan, Chee Seng Chan, Hernán E Aguirre, and Kiyoshi Tanaka. Ceci n’est pas une pipe: A deep convolutional network for fine-art paintings classification. In *2016 IEEE international conference on image processing (ICIP)*, pages 3703–3707. IEEE, 2016.
- [45] Gemini Team, R Anil, S Borgeaud, Y Wu, JB Alayrac, J Yu, R Soricut, J Schalkwyk, AM Dai, A Hauth, et al. Gemini: A family of highly capable multimodal models, 2024. *arXiv preprint arXiv:2312.11805*, 2024.
- [46] Henriikka Vartiainen and Matti Tedre. Using artificial intelligence in craft education: crafting with text-to-image generative models. *Digital Creativity*, 34(1):1–21, 2023.
- [47] Mor Ventura, Eyal Ben-David, Anna Korhonen, and Roi Reichart. Navigating cultural chasms: Exploring and unlocking the cultural pov of text-to-image models. *arXiv preprint arXiv:2310.01929*, 2023.
- [48] Angelina Wang, Vikram V Ramaswamy, and Olga Russakovsky. Towards intersectionality in machine learning: Including more identities, handling underrepresentation, and performing evaluation. In *Proceedings of the 2022 ACM conference on fairness, accountability, and transparency*, pages 336–349, 2022.
- [49] Tobias Weyand, Andre Araujo, Bingyi Cao, and Jack Sim. Google landmarks dataset v2-a large-scale benchmark for instance-level recognition and retrieval. In *Proceedings of the IEEE/CVF conference on computer vision and pattern recognition*, pages 2575–2584, 2020.

- [50] Ben Wills-Eve. *The Role of Automation, Bots and AI in Influencing Knowledge of the Past*. PhD thesis, Lancaster University (United Kingdom), 2023.
- [51] Yankun Wu, Yuta Nakashima, and Noa Garcia. Stable diffusion exposed: Gender bias from prompt to image. In *Proceedings of the AAAI/ACM Conference on AI, Ethics, and Society*, volume 7, pages 1648–1659, 2024.
- [52] Lili Zhang, Xi Liao, Zaijia Yang, Baihang Gao, Chunjie Wang, Qiuling Yang, and Deshun Li. Partiality and misconception: Investigating cultural representativeness in text-to-image models. In *Proceedings of the CHI Conference on Human Factors in Computing Systems*, pages 1–25, 2024.
- [53] Yanzhe Zhang, Lu Jiang, Greg Turk, and Diyi Yang. Auditing gender presentation differences in text-to-image models. In *Proceedings of the 4th ACM Conference on Equity and Access in Algorithms, Mechanisms, and Optimization*, pages 1–10, 2024.

A The HistVis Dataset

Below are all the prompts used in the HistVis-Generated dataset, organized by category.

Music

1. A person listening to music
2. A person performing music
3. A person playing an instrument
4. A person listening to a live performance
5. A person singing

Art

6. A person creating art
7. A person using colors to create something
8. A person admiring an artwork
9. A person sharing their artwork
10. A person sketching something

Communication and Social Interaction

11. A person communicating using a device
12. A person negotiating with someone
13. A person sending a message
14. A person listening to someone speak
15. A person spreading a rumor

Family and Relationships

16. A person spending time with their family
17. A person laughing with a friend
18. A person holding hands with a loved one
19. A person embracing their child
20. A person welcoming a loved one home

Transportation and Travel

21. A person traveling from one place to another
22. A person waiting for a ride
23. A person carrying belongings during a journey
24. A person navigating using a device
25. A person preparing for a journey

Urban Life

26. A person carrying shopping bags
27. A person walking through a market
28. A person navigating through a street
29. A person waiting at a public gathering spot
30. A person enjoying food from a street vendor

Physical and Recreational Activities

31. A person dancing with someone
32. A person running
33. A person playing a game with someone
34. A person discovering a new toy
35. A person exercising

Cooking and Dining

36. A person sharing a meal with another
37. A person cooking dinner
38. A person setting a table
39. A person drinking from a bottle
40. A person holding a bowl of food

Daily Chores and Activities

41. A person cleaning with a tool
42. A person washing laundry
43. A person organizing items in a bag
44. A person feeding an animal
45. A person ironing clothes

Craftsmanship and Labor

46. A person observing a building under construction
47. A person repairing an object
48. A person making clothes
49. A person building a shelter
50. A person painting a surface

Religion and Spirituality

51. A person praying
52. A person celebrating a religious event
53. A person reading a sacred text
54. A person lighting a candle in a place of worship
55. A person meditating quietly

Celebration and Festivities

56. A person unwrapping a gift
57. A person dancing during a festival
58. A person toasting with a glass at a celebration
59. A person cheering at a celebration
60. A person decorating a space for a celebration

Survival and Comfort

61. A person using a tool to illuminate a dark space
62. A person lighting a fire
63. A person gathering water from a natural source
64. A person shielding themselves from rain
65. A person shielding their eyes from the sun

Health and Well-being

66. A person taking medicine
67. A person examining a patient
68. A person assisting someone who is injured
69. A person treating a wound with care
70. A person applying a medical treatment

Education and Learning

71. A person studying
72. A person teaching music to another
73. A person guiding someone in understanding
74. A person using a learning tool
75. A person reading and taking notes

Agriculture

- 76. A person planting seeds in the ground
- 77. A person tending a vegetable garden
- 78. A person caring for livestock
- 79. A person watering crops
- 80. A person plowing a field

Fashion and Personal Care

- 81. A person putting on clothing
- 82. A person showing off their style
- 83. A person accessorizing their outfit
- 84. A person shaving their face
- 85. A person combing their hair

Emotion and Personal Traits

- 86. A person showing bravery
- 87. A person expressing joy after achieving a goal
- 88. A person smiling warmly at a friend
- 89. A person expressing gratitude to another
- 90. A person standing up for a cause

Work and Collaboration

- 91. A person working
- 92. A person organizing their work equipment
- 93. A person reviewing a group's progress on a work-related task
- 94. A person assisting a coworker with a challenge
- 95. A person preparing for a day of work

Commerce

- 96. A person selling items at a market stall
- 97. A person bargaining with a vendor
- 98. A person wrapping goods for a customer
- 99. A person opening a shop
- 100. A person closing a register after a sale

B CNN training on Wikiart data

We evaluate four fine-tuning strategies for visual style prediction: (i) unfreezing all layers, (ii) freezing only the first layer, (iii) freezing the first two layers, and (iv) training only the classification head while keeping the base model frozen. All images are resized to 224×224 pixels and normalized to $[0, 1]$ by scaling pixel values by $1/255$. To enhance generalization and mitigate overfitting, we apply data augmentation, including random rotations (up to 20°), translations (10%), shear and zoom transformations (10%), and horizontal flipping.

Training Configuration All models are trained using the Adam optimizer with a learning rate of 1×10^{-3} and categorical cross-entropy loss. We train for a maximum of 50 epochs with a batch size of 32 on a single NVIDIA A100 GPU. To ensure robust convergence and prevent overfitting, we employ early stopping based on validation loss (patience of 5 epochs, with best weights restored), learning rate reduction on plateau (factor of 0.5, patience of 3, minimum learning rate of 1×10^{-6}), and checkpointing to retain the best-performing model on the validation set. For reproducibility, we fix the random seed to 42 across both NumPy and TensorFlow.

Classification Report Table 2 presents the per-class classification performance of the best-performing fine-tuning strategy. The table reports Precision, Recall, and F1-score for each of the six art medium categories, demonstrating high classification accuracy across all classes, with particularly strong performance for paintings (F1-score: 0.94) and illustrations (F1-score: 0.88). The results indicate that the model effectively differentiates between artistic styles, supporting its reliability for analyzing implicit stylistic associations in historical image generation.

Table 2: Per-class classification performance of the best-performing fine-tuning strategy for art medium classification

Class	Precision	Recall	F1-score
Drawings	0.79	0.86	0.82
Engraving	0.84	0.82	0.83
Illustrations	0.90	0.86	0.88
Painting	0.95	0.93	0.94
Photography	0.88	0.83	0.85

B.1 Predicted visual styles

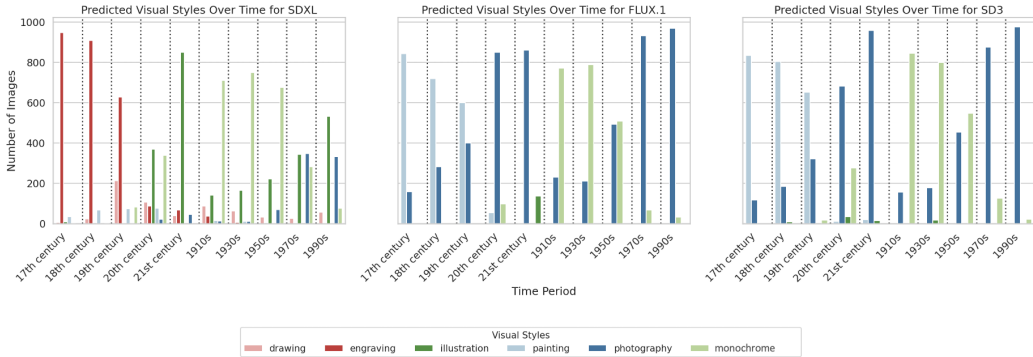


Figure 7: Predicted visual styles of generated images across different historical periods for each TTI model. Each historical period is evaluated using 1,000 generated images per model.

Figure 7 presents the predicted stylistic properties of generated images across time periods \mathcal{T} for each TTI model. Even though no explicit stylistic instructions were provided in the prompts, models exhibit consistent yet model-specific stylistic tendencies. For instance, SDXL predominantly generates engraving-like images for the 17th and 18th centuries (e.g., 947 of 1,000 images for the 17th century, 909 for the 18th), while SD3 and FLUX.1 favor painting-like renderings for these same

periods. In the 20th and 21st centuries, SD3 and FLUX.1 predominantly generate photography-like images, whereas SDXL exhibits greater stylistic diversity, generating illustrations, drawings, engravings and some photography. More specifically, in the 1910s, 1930s, and 1950s, SD3 and FLUX.1 mostly generate b&w photographs, reinforcing the historical association of these decades with monochrome photography. In contrast, SDXL produces a wider variety of styles, including illustrations and engravings, even when generating images for the same time periods. These results indicate that TTI models encode implicit associations between historical periods and specific stylistic renderings, which emerge even when no style is specified in the prompt, raising important questions about how generative models learn and internalize visual conventions from their training data.

Example Outputs The examples illustrated in Figure 8 illustrate how TTI models implicitly associate specific stylistic patterns with historical periods. Rather than generating images solely based on the historical context in the prompt, they impose learned stylistic conventions, even when no explicit artistic style is specified.

- **A person showing off their style in the:**
 - **17th Century** - Paintings (SD3)
 - **18th Century** – Engravings (SDXL)
 - **1990s** – Photography (FLUX.1)

- **A person teaching music to another in the:**
 - **19th Century** – Paintings (SD3)
 - **21st Century** – Illustrations (SDXL)
 - **1910s** - Monochrome Photography (FLUX.1)

- **A person embracing their child in the:**
 - **19th Century** – Drawings (SDXL)
 - **19th Century** - Paintings (SD3)
 - **20th Century** - Monochrome Photography (FLUX.1)

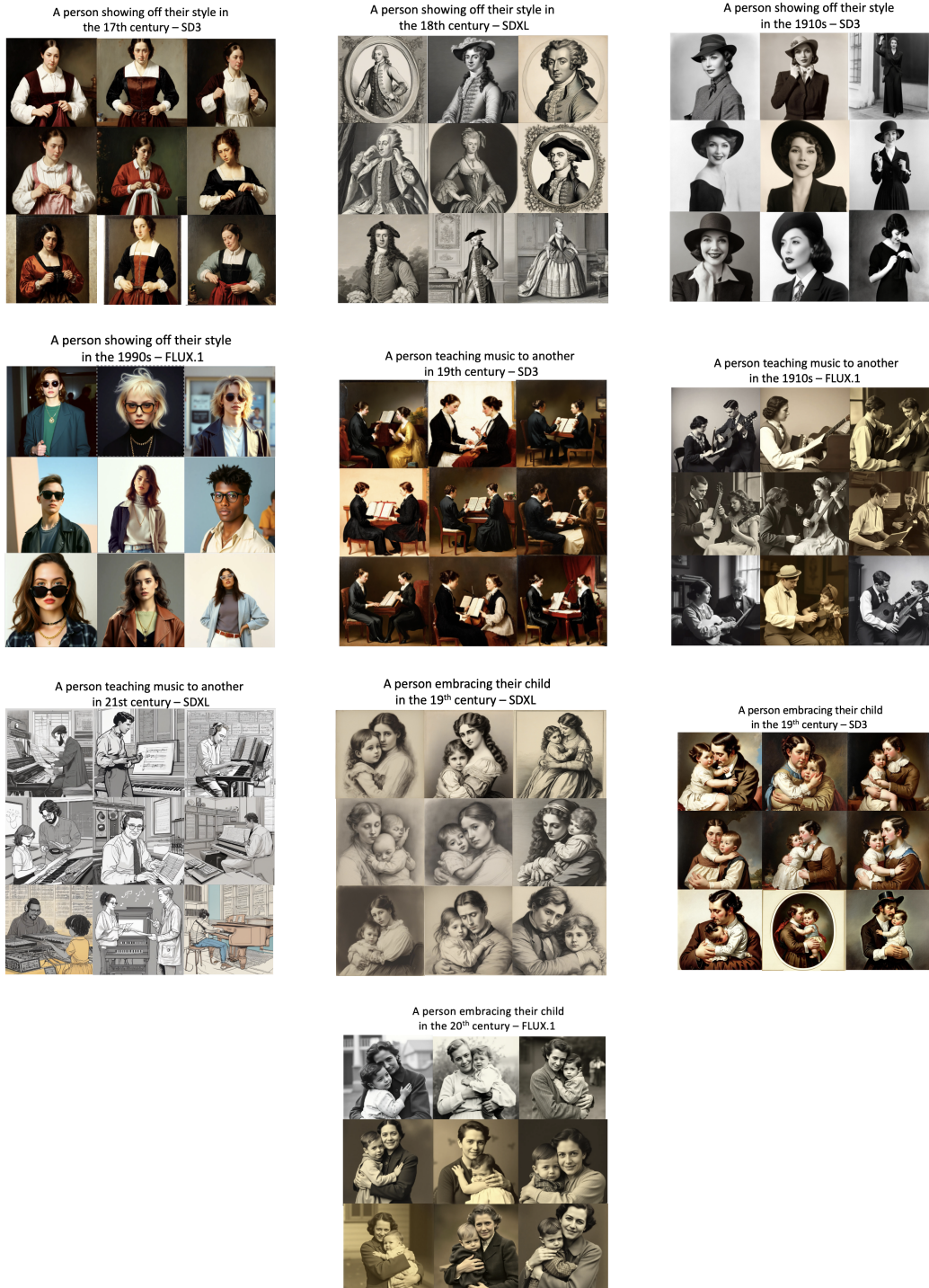


Figure 8: Examples of visual outputs across styles, activities, and time periods.

C Visual Bias Mitigation and Additional Qualitative Examples

Prompt engineering has been explored as a bias mitigation strategy in both text and image generation, with studies demonstrating its effectiveness in reducing demographic biases in LLMs and guiding TTI models toward more balanced outputs [10, 14]. Taking that into consideration, we examined whether the implicit stylistic tendencies of SDXL, which exhibited the most diverse associations

across historical periods (e.g., engravings for the 17th and 18th centuries, drawings for the 19th century, and illustrations for the 21st century), could be adjusted through targeted prompt engineering. Specifically, we replaced the standard neutral prompt (e.g., “A person [activity] in the [time period]”) with a more explicit instruction (“A photorealistic image of [activity] in the [historical period]”). Additionally, we introduced a negative prompt (“black and white image”) to discourage monochrome outputs by applying negative weights, a common practice in diffusion-based TTI models to steer the generation process away from unwanted elements [2]. The effectiveness of these modifications was then evaluated using our trained CNN to predict the visual styles of the newly generated images.

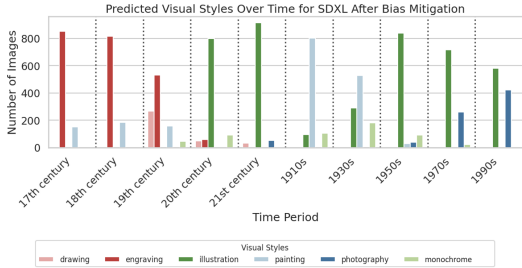


Figure 9: Predicted visual styles of SDXL-generated images across different historical periods after applying bias mitigation via prompt engineering. Each historical period is evaluated using 1,000 generated images.

Interpretation. Table 3 reveals that prompt-level mitigation has a statistically significant effect on the stylistic dominance of SDXL outputs across all evaluated periods. In earlier centuries (17th–19th), VSD scores decrease, indicating a reduction in stylistic convergence. However, in most 20th-century decades, especially the 1970s and 20th century aggregate, VSD scores increase substantially, suggesting a shift toward a new dominant style—typically illustration. While mitigation successfully disrupts certain stylistic defaults (e.g., monochrome in the 1930s), it also introduces or reinforces others, highlighting the persistence and asymmetry of stylistic biases in text-to-image generation.

Period	Model	Before	After	Δ VSD	95% CI	<i>p</i> -value
17th c.	SDXL	0.95	0.85	−0.10***	[−0.13, −0.07]	< .0001
18th c.	SDXL	0.91	0.82	−0.09***	[−0.12, −0.06]	< .0001
19th c.	SDXL	0.63	0.53	−0.10***	[−0.14, −0.06]	< .0001
20th c.	SDXL	0.37	0.80	+0.43***	[+0.39, +0.47]	< .0001
21st c.	SDXL	0.85	0.92	+0.07***	[+0.04, +0.10]	< .0001
1910s	SDXL	0.71	0.80	+0.09***	[+0.05, +0.13]	< .0001
1930s	SDXL	0.75	0.53	−0.22***	[−0.26, −0.18]	< .0001
1950s	SDXL	0.68	0.84	+0.16***	[+0.12, +0.20]	< .0001
1970s	SDXL	0.35	0.72	+0.37***	[+0.33, +0.41]	< .0001
1990s	SDXL	0.52	0.58	+0.06**	[+0.02, +0.10]	0.0070

Table 3: Visual Style Dominance (VSD) scores for SDXL before and after prompt-level mitigation across historical periods. Δ VSD reflects the change in dominance (After–Before). All changes are statistically significant after FDR correction. Significance levels: *** $p < 0.001$, ** $p < 0.01$.

Figure 9 shows the visual predictions of SDXL images after applying bias mitigation through targeted prompt engineering. Even when explicitly prompting for “photorealistic images,” the distribution of stylistic outputs at the century level remains largely unchanged. SDXL continues to predominantly generate engraving-like images in the 17th, 18th and 19th century, suggesting that its deep-rooted historical stylistic associations are not easily overridden by prompt modifications alone. At the decade level, however, some shifts are observed. Notably, the proportion of monochrome images decreases following bias mitigation. Yet, rather than transitioning toward color photography as one might expect, SDXL instead increases the generation of paintings and illustrations. These results indicate that while prompt-level interventions can partially influence stylistic biases at a more granular level, such as reducing the proportion of monochrome outputs, they remain insufficient to fully counteract the model’s learned stylistic tendencies. Figures 10 and 11 illustrate how certain visual styles either persist or shift following the application of the bias mitigation approach.

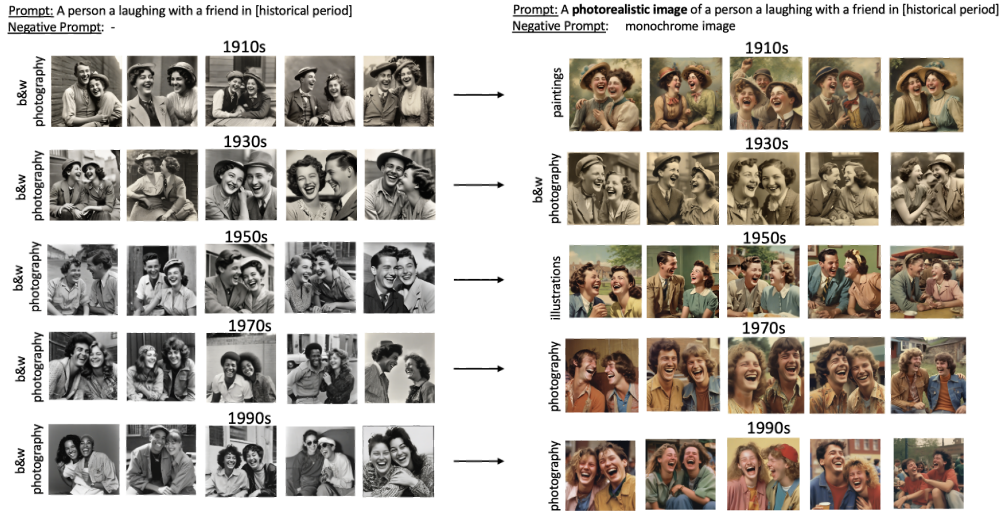


Figure 10: Predicted visual styles of generated images derived from the prompt “A person laughing with a friend in the [historical period]” (left) and “A photorealistic image of a person laughing with a friend in the [historical period]” (right) with "monochrome picture" used as a negative prompt.

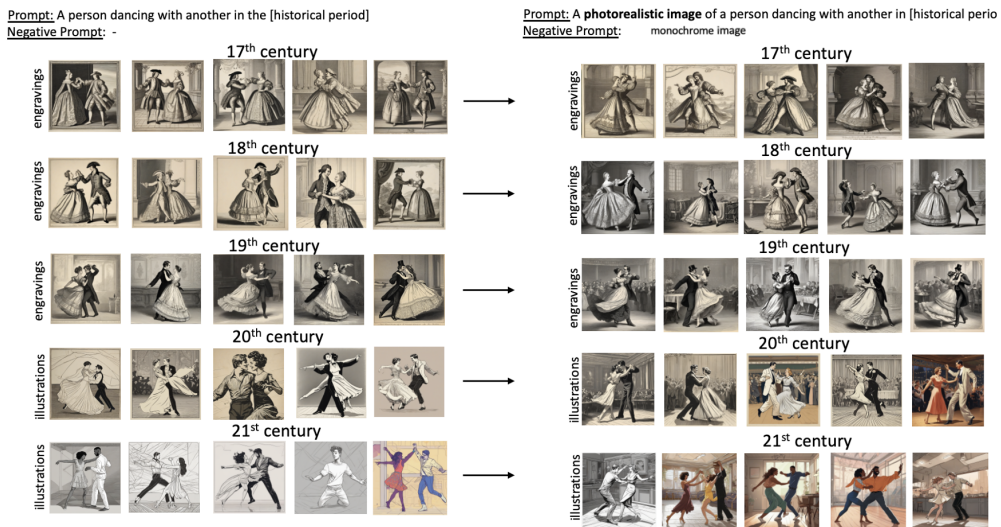


Figure 11: Predicted visual styles of generated images derived from the prompt “A person dancing with another in the [historical period]” (left) and “A photorealistic image of a person dancing with another in the [historical period]” (right) with "monochrome picture" used as a negative prompt.

D LLM Input for Anachronism Detection

Anachronism Identification: You will be provided with a list of prompts describing people engaged in specific activities during various historical time periods. These prompts will serve as input for a Text-to-Image Generative Model like Stable Diffusion. Based on each prompt, perform the following tasks:

- Identify potential anachronisms that might appear in the generated image. Ensure that the list is relevant to the activity, time period, and setting described in the prompt.
- For each identified anachronism, generate a question to determine whether the anachronism appears in the generated image. Each question should end with: *‘Answer with ‘yes’ (if the anachronism is present) or ‘no’ (if it is absent).’*

All answers must be in json format.

Example JSON Representation:

Listing 1: Example JSON structure for anachronism detection

```

1 {
2   "index": 1,
3   "prompt": "A person listening to music in the 19th century",
4   "possible_anachronisms": [
5     "modern music devices",
6     "modern clothing",
7     "modern surroundings"
8   ],
9   "questions_to_identify_anachronisms": {
10    "modern music devices": "Is the person using modern music devices, such as headphones
11    or smartphones that didn't exist in the 19th century? Answer with 'yes' or 'no'
12    '.",
13    "modern clothing": "Is the person wearing modern clothing styles not typical for the
14    19th century? Answer with 'yes' or 'no'."
15    "modern surroundings": "Are there modern surroundings in the image, such as
16    skyscrapers, cars, or items that didn't exist in the 19th century? Answer with '
17    yes' or 'no'."
18  }
19 }

```

E Anachronism Frequency & Severity Results

Anachronism Frequency and Severity by Decade Figure 12 plots the top 15 anachronistic elements per model, ranked by *frequency* and *severity*, and aggregated across different decades rather than centuries. Each point corresponds to an element proposed by the LLM and verified via VQA, with fuzzy matching used to unify lexical variations. Items like *clothing* continue to appear more frequently than they do severely (7-10%), whereas elements such as *audio devices* are comparatively rare but exhibit higher severity, once generated, they strongly conflict with the historical context. This pattern again illustrates that the models rely heavily on conceptual cues (e.g., “audio sources” for music-related prompts), often at the expense of accurate temporal conditioning.

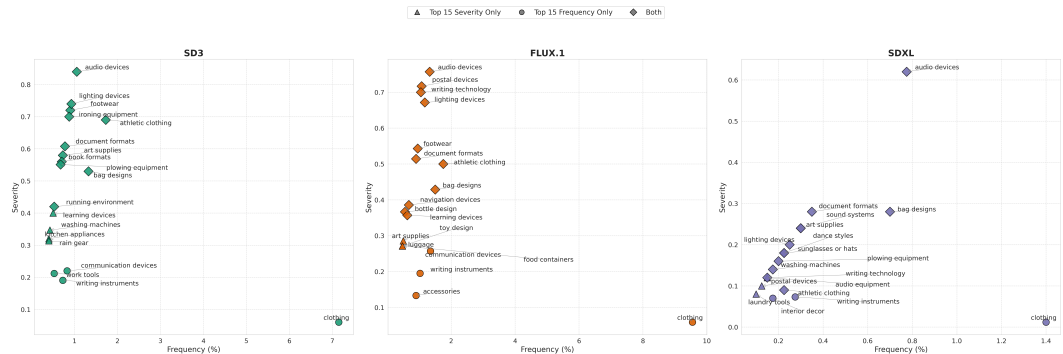
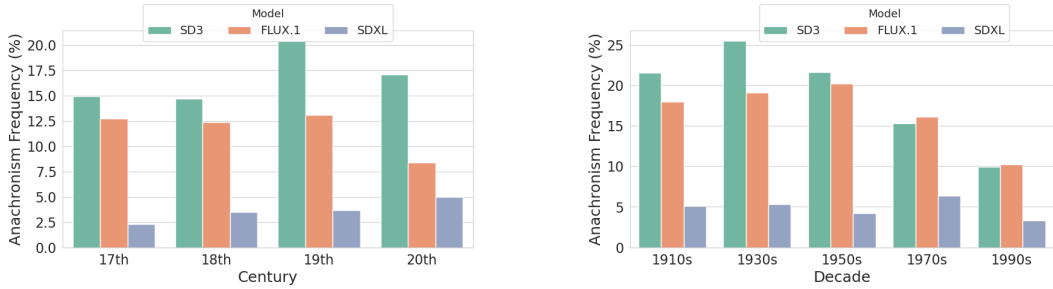


Figure 12: Top 15 anachronistic elements per model, aggregated across all decades, ranked by *frequency* (x-axis) and *severity* (y-axis). Circles indicate elements in the top 15 by frequency only, triangles by severity only, and diamonds appear in the top 15 of both.

Overall Anachronism Frequency To assess each model’s overall anachronistic tendency across historical periods, we measure the overall anachronism rate, defined as the proportion of images containing at least one detected anachronism. The frequency of specific anachronisms across centuries and decades for each model is illustrated in Figure 13. The 21st century is excluded as anachronisms cannot be meaningfully defined. By century, SD3’s anachronism frequency increases from 15% in the 17th and 18th centuries to over 20% in the 19th century, then decreases to 17% in the 20th. FLUX.1 remains stable at 12–13%, while SDXL stays below 5%, with a slight uptick in the 20th century.

By decade, SD3 peaks at 25% in the 1930s before falling to 10% in the 1990s. FLUX.1 follows a similar but milder trend, while SDXL remains consistently low (3.3–6.4%). These results suggest that while all models generate anachronisms, SD3 does so most frequently, especially in earlier periods. FLUX.1 remains stable, improving over time, while SDXL has the highest historical accuracy.



(a) Anachronism **frequency** across **centuries**. Each bar shows the percentage of images with at least one anachronism per model per century.

(b) Anachronism **frequency** across **decades**. Each bar shows the percentage of images with at least one anachronism per model per decade.

Figure 13: Anachronism frequency for each TTI model, grouped by centuries (left) and decades (right). Each model was evaluated on 1,000 images per period, totaling 4,000 per century and 5,000 per decade.

E.1 Anachronism Severity and Frequency Scores per Model and Historical Period

Anachronism	FLUX.1		SD3		SDXL	
	Freq.(%)	Sev.	Freq.(%)	Sev.	Freq.(%)	Sev.
Clothing	0.45	0.015	0.725	0.032	0.075	0.003
Bag Designs	0.325	0.65	0.475	1.0	0.075	0.15
Audio Devices	0.0	0.0	0.125	0.5	0.125	0.5
Communication Devices	0.225	0.3	0.1	0.133	0.0	0.0
Ironing Equipment	0.175	0.7	0.25	1.0	0.05	0.2
Bottle Design	0.25	1.0	0.175	0.7	0.025	0.1
Food Containers	0.15	0.6	0.2	0.8	0.0	0.0
Lighting Devices	0.1	0.2	0.075	0.3	0.05	0.2
Vendor Setup	0.15	0.6	0.225	0.9	0.0	0.0
Art Supplies	0.2	0.4	0.125	0.5	0.025	0.1
Sound Equipment	0.175	0.7	0.075	0.3	0.0	0.0
Writing Instruments	0.175	0.233	0.075	0.1	0.0	0.0
Gallery Setting	0.175	0.35	0.075	0.333	0.075	0.3
Gift Wrapping Materials	0.15	0.6	0.0	0.0	0.025	0.1
Rain Gear	0.175	0.35	0.15	0.6	0.05	0.2
Ambient Lighting	0.1	0.4	0.075	0.3	0.0	0.0
Postal Devices	0.075	0.3	0.075	0.3	0.0	0.0
Athletic Clothing	0.0	0.0	0.025	0.05	0.0	0.0
Writing Technology	0.075	0.3	0.075	0.3	0.0	0.0
Pharmaceutical Packaging	0.075	0.15	0.075	0.3	0.0	0.0
Building Materials	0.05	0.2	0.125	0.5	0.025	0.1
Learning Devices	0.0	0.0	0.0	0.0	0.0	0.0
Maps or Interfaces	0.0	0.0	0.0	0.0	0.0	0.0
Navigating Devices	0.0	0.05	0.0	0.0	0.0	0.0
Running Environment	0.0	0.0	0.0	0.0	0.0	0.0
Street Fixtures	0.075	0.3	0.0	0.0	0.0	0.0
Toy Design	0.05	0.2	0.05	0.2	0.0	0.0
Watering Equipment	0.075	0.15	0.05	0.2	0.0	0.0

Table 4: 17th Century Anachronism Scores

Anachronism	FLUX.1		SD3		SDXL	
	Freq.(%)	Sev.	Freq.(%)	Sev.	Freq.(%)	Sev.
Clothing	0.850	0.036	2.225	0.094	0.250	0.011
Bag Designs	0.275	0.55	0.400	0.80	0.125	0.00
Audio Devices	0.075	0.30	0.200	1.0	0.200	0.00
Communication Devices	0.225	0.30	0.175	0.233	0.000	0.00
Ironing Equipment	0.025	0.10	0.200	1.0	0.050	0.20
Bottle Design	0.175	0.70	0.050	0.20	0.025	0.10
Food Containers	0.150	0.60	0.100	0.40	0.000	0.00
Lighting Devices	0.100	0.40	0.125	0.50	0.050	0.20
Vendor Setup	0.100	0.40	0.100	0.40	0.000	0.00
Art Supplies	0.075	0.30	0.050	0.20	0.100	0.40
Sound Equipment	0.200	0.80	0.075	0.30	0.000	0.00
Writing Instruments	0.075	0.10	0.125	0.50	0.000	0.00
Gallery Setting	0.100	0.10	0.075	0.30	0.025	0.10
Gift Wrapping Materials	0.050	0.20	0.175	0.70	0.025	0.10
Rain Gear	0.100	0.40	0.100	0.40	0.000	0.00
Ambient Lighting	0.100	0.40	0.125	0.50	0.000	0.00
Postal Devices	0.200	0.80	0.050	0.20	0.000	0.00
Athletic Clothing	0.050	0.10	0.250	0.50	0.000	0.00
Writing Technology	0.200	0.80	0.000	0.00	0.000	0.00
Pharmaceutical Packaging	0.000	0.00	0.125	0.50	0.000	0.00
Building Materials	0.025	0.10	0.125	0.50	0.050	0.20
Learning Devices	0.000	0.00	0.100	0.40	0.000	0.00
Maps or Interfaces	0.000	0.00	0.025	0.025	0.000	0.00
Navigation Devices	0.000	0.00	0.025	0.10	0.000	0.00
Running Environment	0.000	0.00	0.050	0.20	0.000	0.00
Street Fixtures	0.025	0.10	0.025	0.10	0.050	0.20
Toy Design	0.000	0.00	0.075	0.30	0.025	0.10
Watering Equipment	0.025	0.10	0.025	0.10	0.025	0.10

Table 6: 19th Century Anachronism Scores

Anachronism	FLUX.1		SD3		SDXL	
	Freq.(%)	Sev.	Freq.(%)	Sev.	Freq.(%)	Sev.
Clothing	0.350	0.015	0.625	0.026	0.075	0.003
Bag Designs	0.325	0.65	0.425	0.85	0.100	0.20
Audio Devices	0.000	0.00	0.175	0.70	0.225	1.0
Communication Devices	0.200	0.267	0.175	0.233	0.000	0.00
Ironing Equipment	0.025	0.10	0.225	1.0	0.025	0.10
Bottle Design	0.200	0.80	0.050	0.20	0.050	0.20
Food Containers	0.150	0.60	0.200	0.80	0.000	0.00
Lighting Devices	0.100	0.40	0.125	0.50	0.050	0.20
Vendor Setup	0.100	0.40	0.100	0.40	0.000	0.00
Art Supplies	0.075	0.30	0.050	0.20	0.100	0.40
Sound Equipment	0.200	0.80	0.075	0.30	0.000	0.00
Writing Instruments	0.075	0.10	0.125	0.50	0.000	0.00
Gallery Setting	0.100	0.10	0.075	0.30	0.025	0.10
Gift Wrapping Materials	0.050	0.20	0.175	0.70	0.025	0.10
Rain Gear	0.100	0.40	0.100	0.40	0.000	0.00
Ambient Lighting	0.100	0.40	0.125	0.50	0.000	0.00
Postal Devices	0.200	0.80	0.050	0.20	0.000	0.00
Athletic Clothing	0.000	0.00	0.125	0.50	0.000	0.00
Writing Technology	0.025	0.10	0.125	0.50	0.050	0.20
Pharmaceutical Packaging	0.000	0.00	0.100	0.40	0.000	0.00
Building Materials	0.000	0.00	0.025	0.025	0.000	0.00
Learning Devices	0.000	0.00	0.025	0.10	0.000	0.00
Maps or Interfaces	0.000	0.00	0.050	0.20	0.000	0.00
Navigating Devices	0.025	0.10	0.025	0.10	0.050	0.20
Running Environment	0.000	0.00	0.075	0.30	0.025	0.10
Street Fixtures	0.025	0.10	0.025	0.10	0.025	0.10

Table 5: 18th Century Anachronism Scores

Anachronism	FLUX.1		SD3		SDXL	
	Freq.(%)	Sev.	Freq.(%)	Sev.	Freq.(%)	Sev.
Clothing	0.400	0.017	0.725	0.031	0.125	0.005
Bag Designs	0.225	0.45	0.300	0.60	0.175	0.35
Audio Devices	0.225	0.90	0.225	0.90	0.150	0.60
Communication Devices	0.150	0.20	0.100	0.133	0.050	0.067
Ironing Equipment	0.075	0.30	0.175	0.70	0.050	0.20
Bottle Design	0.075	0.30	0.100	0.40	0.000	0.00
Food Containers	0.075	0.30	0.100	0.40	0.000	0.00
Lighting Devices	0.150	0.60	0.200	0.80	0.000	0.00
Vendor Setup	0.075	0.30	0.100	0.40	0.000	0.00
Art Supplies	0.025	0.10	0.000	0.00	0.000	0.00
Sound Equipment	0.025	0.10	0.050	0.20	0.000	0.00
Writing Instruments	0.025	0.10	0.050	0.20	0.000	0.00
Gallery Setting	0.025	0.033	0.125	0.167	0.000	0.00
Gift Wrapping Materials	0.025	0.10	0.050	0.20	0.075	0.30
Rain Gear	0.000	0.00	0.000	0.00	0.000	0.00
Ambient Lighting	0.000	0.00	0.000	0.00	0.000	0.00
Postal Devices	0.025	0.10	0.000	0.00	0.000	0.00
Athletic Clothing	0.025	0.05	0.225	0.45	0.000	0.00
Writing Technology	0.025	0.10	0.000	0.00	0.025	0.10
Pharmaceutical Packaging	0.075	0.30	0.050	0.20	0.000	0.00
Building Materials	0.000	0.00	0.000	0.00	0.000	0.00
Learning Devices	0.050	0.20	0.225	0.90	0.075	0.30
Maps or Interfaces	0.050	0.20	0.250	1.00	0.125	0.50
Navigation Devices	0.075	0.30	0.250	1.00	0.125	0.50
Running Environment	0.075	0.30	0.100	0.40	0.025	0.10
Street Fixtures	0.025	0.10	0.025	0.10	0.000	0.00
Toy Design	0.075	0.30	0.025	0.10	0.000	0.00
Watering Equipment	0.000	0.00	0.000	0.00	0.000	0.00

Table 7: 20th Century Anachronism Scores

F Example Outputs of Severe Anachronisms

A person carrying shopping bags in the 17th century – SD3



(a) Modern shopping bags

A person cooking dinner in the 17th century – SD3.



(b) Modern cooking tool

A person ironing in the 18th century – SD3



(c) Modern ironing equipment

A person singing in the 19th century – FLUX.1



(d) Modern audio device

A person using a communication device in the 20th century – FLUX.1



(e) Modern communication device

A person listening to music in the 18th century – SD3



(f) Modern audio device

A person communicating using a device in the 1950s – FLUX.1



(g) Modern communication device

A person using a learning tool in the 1930s – SD3



(h) Modern learning tool

A person communicating using a navigation Device in the 1990s – FLUX.1



(i) Modern navigation device

Figure 14: Examples of generated images depicting universal human activities across different historical periods, highlighting instances of high-severity anachronisms.

G User Study

Figure 15 presents the user interface for the human evaluation study, which includes the task description given to participants and example questions. The task description introduces the concept of anachronisms to ensure participants understand it before beginning the task and provides illustrative examples of both historically accurate and anachronistic images for further clarification. Participants were then required to assess TTI-generated images for temporal inconsistencies by answering a series of yes-no questions.

Identify Anachronisms in AI Generated Images

Task Description: In this task, you will evaluate images that have been AI-generated to represent different historical realities, such as centuries (e.g. 17th century, 18th century) or decades (e.g. 1910s, 1950s, etc.). Please note that these images are AI-generated and are not genuine historical photographs. Your task is to identify the existence of anachronisms given the conditioned time period.

What is an anachronism? An anachronism is something that is out of place in terms of time—for example, a modern object or style appearing in a historical setting where it does not belong.

Examples

<p>Example with Anachronisms (Yes)</p>  <p>A person ironing clothes in the 18th century (modern ironing board present)</p>	<p>Example without Anachronisms (No)</p>  <p>A person spending time with their family in the 18th century (historically accurate)</p>	 <p>Description: A person listening to music in the 17th century Question: Is there an anachronism in the picture? Answer with "Yes" or "No".</p> <p><input type="radio"/> Yes <input type="radio"/> No <input type="button" value="Next"/></p>
 <p>Description: A person waiting for a ride in the 17th century Question: Is there an anachronism in the picture? Answer with "Yes" or "No".</p> <p><input type="radio"/> Yes <input type="radio"/> No <input type="button" value="Next"/></p>	 <p>Description: A person accessorizing their outfit in the 17th century Question: Is there an anachronism in the picture? Answer with "Yes" or "No".</p> <p><input type="radio"/> Yes <input type="radio"/> No <input type="button" value="Next"/></p>	 <p>Description: A person laughing with a friend in the 17th century Question: Is there an anachronism in the picture? Answer with "Yes" or "No".</p> <p><input type="radio"/> Yes <input type="radio"/> No <input type="button" value="Next"/></p>

Figure 15: User interface for the human evaluation study, presenting the task description given to participants along with example questions. The interface explains anachronisms, provides illustrative examples of historically accurate and anachronistic images, and includes yes-no questions for assessing temporal inconsistencies in TTI-generated images.

H Demographic Representation

H.1 LLM Input for Demographic Prediction

For a given activity and historical period described in the prompt, estimate the plausible demographic breakdown based on global historical context:

- **Gender:(%)** Proportion of male and female participants
- **Race:(%)** Estimated distribution across the following categories: White, Black, Asian, Indian, East Asian, Southeast Asian, and Middle Eastern.

The estimates should be informed by historical social structures, legal constraints, cultural practices, and prevailing social hierarchies. Avoid focusing on a specific geographic region (e.g., Europe); instead, consider patterns and norms that shaped access and participation globally across different societies.

H.2 FairFace-Derived Demographic Outputs

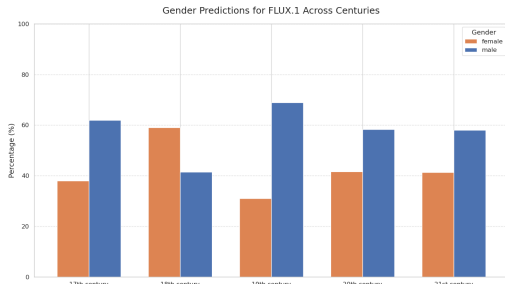
We analyze the face classifier predictions from the three TTI models $\mathbf{m} \in \{\text{SDXL}, \text{SD3}, \text{FLUX.1}\}$ to understand the distributions they produce before comparing them to GPT-4o’s estimates. Out of 30,000 generated images, 1,221 (4.07%) were excluded due to low classifier confidence, often because the faces were blurred or unclear.

Comparison to DeepFace’s Predictions To assess FairFace’s consistency, we sampled 5,000 images (500 per time period/model pair) and found that FairFace and DeepFace agreed on gender 95.9% of the time ($\kappa = 0.93$) and on race 90.8% of the time ($\kappa = 0.83$). To align FairFace’s seven race categories with DeepFace’s single ‘Asian’ label, we aggregated FairFace’s ‘East Asian’ and ‘Southeast Asian’ predictions into one ‘Asian’ category. All other FairFace labels map directly. After this, we computed the per-class agreement rates and Cohen’s κ between the two face classifiers reported in Table 8.

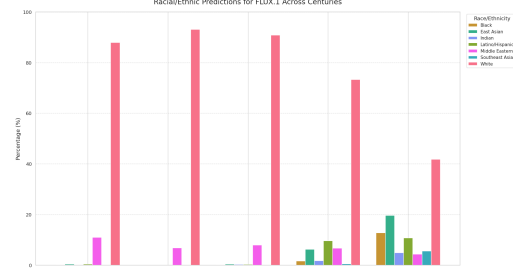
Table 8: Per-class agreement rates and Cohen’s κ between FairFace and DeepFace (post-aggregation).

Category	Percent agreement (%)	Cohen’s κ
White	93.0	0.85
Black	94.5	0.87
Indian	87.2	0.75
Asian	92.0	0.88
Middle Eastern	88.8	0.80
Latino	89.0	0.81
Male	95.6	0.92
Female	96.2	0.93

Face Classifier Predictions Examining these classifier-derived outputs reveals that demographic patterns vary across models. As shown in the barplots below, SDXL primarily generates male figures in earlier centuries (e.g., 70 women versus 930 men in the 17th century), while SD3, in contrast, produces more female figures in certain decades, such as the 1950s (700 female versus 300 male). Across all models, white individuals are overwhelmingly depicted in earlier periods, with racial diversity increasing only after the 20th century, indicating potential biases in how different models represent historical demographics.

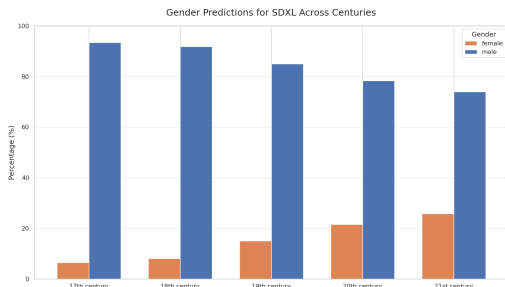


(a) Gender distribution across centuries (FLUX.1)

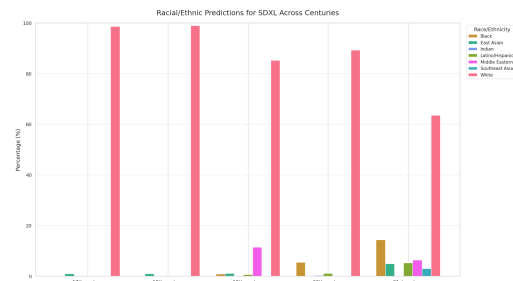


(b) Race distribution across centuries (FLUX.1)

Figure 16: Demographic breakdowns (FairFace predictions) across centuries for **FLUX.1**.

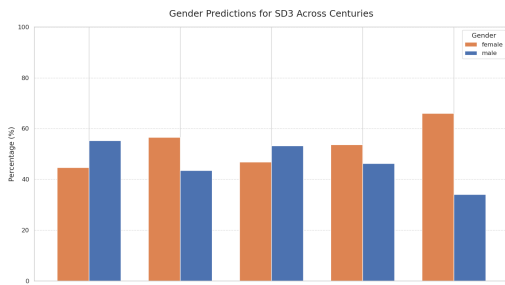


(a) Gender distribution across centuries (SDXL)

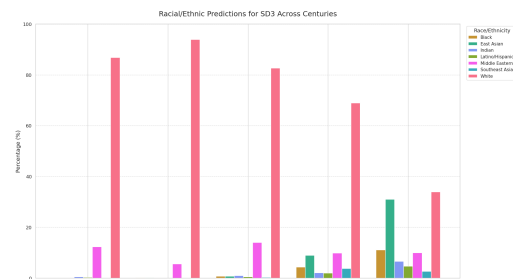


(b) Race distribution across centuries (SDXL)

Figure 17: Demographic breakdowns (FairFace predictions) across centuries for **SDXL**.

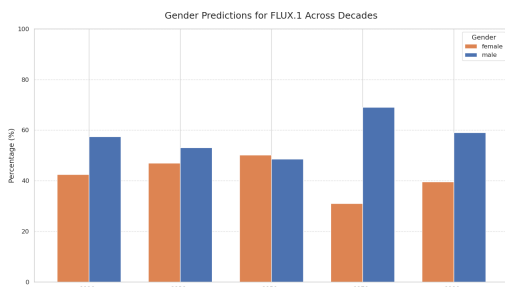


(a) Gender distribution across centuries (SD3)

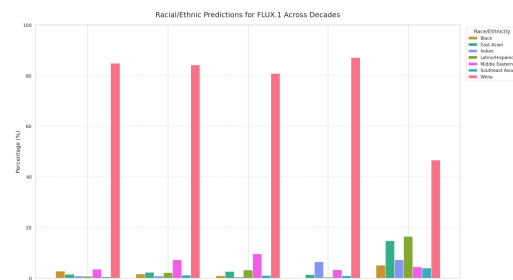


(b) Race distribution across centuries (SD3)

Figure 18: Demographic breakdowns (FairFace predictions) across centuries for **SD3**.

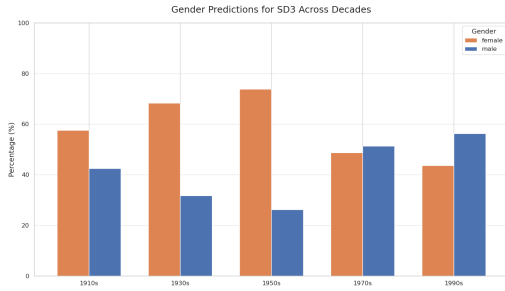


(a) Gender distribution across decades (FLUX.1)

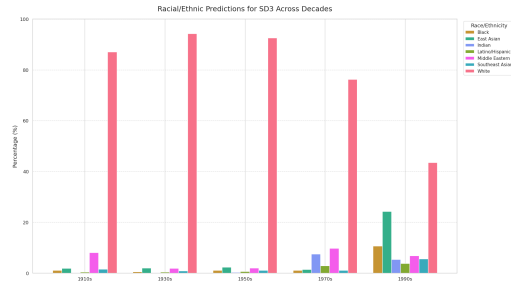


(b) Race distribution across decades (FLUX.1)

Figure 19: Demographic breakdowns (FairFace predictions) across decades for **FLUX.1**.

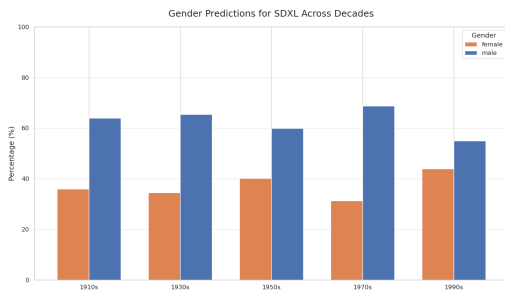


(a) Gender distribution across decades (SD3)

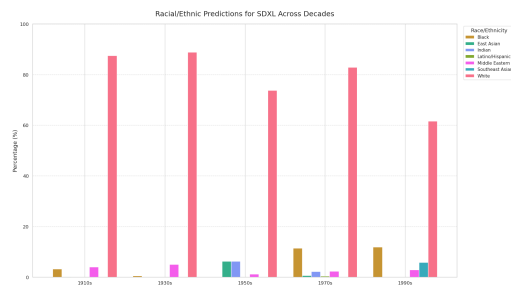


(b) Race distribution across decades (SD3)

Figure 20: Demographic breakdowns (FairFace predictions) across decades for **SD3**.



(a) Gender distribution across decades (SDXL)



(b) Race distribution across decades (SDXL)

Figure 21: Demographic breakdowns (FairFace predictions) across decades for **SDXL**.

H.3 Gender and Racial Over-Underrepresentation Values

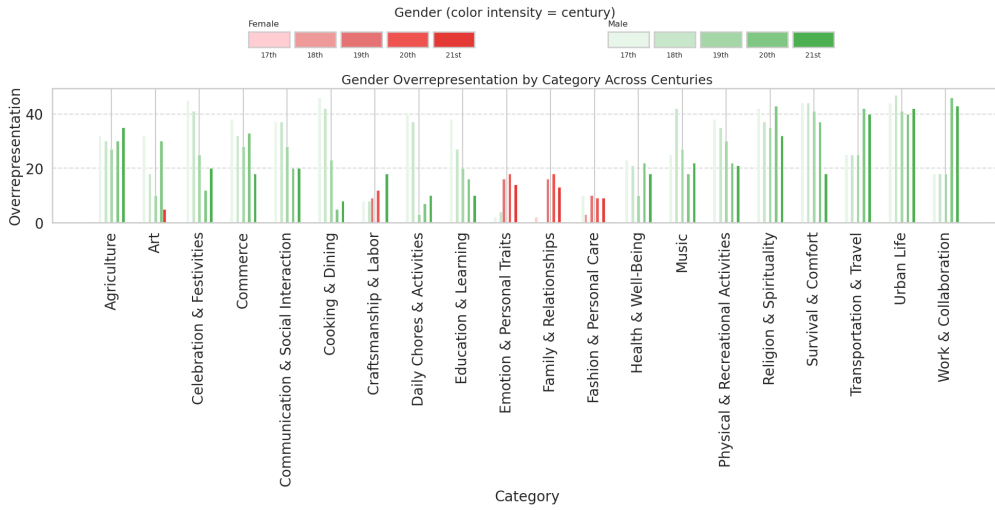


Figure 22: Over- and underrepresentation of gender predictions across **centuries** for **SDXL**.

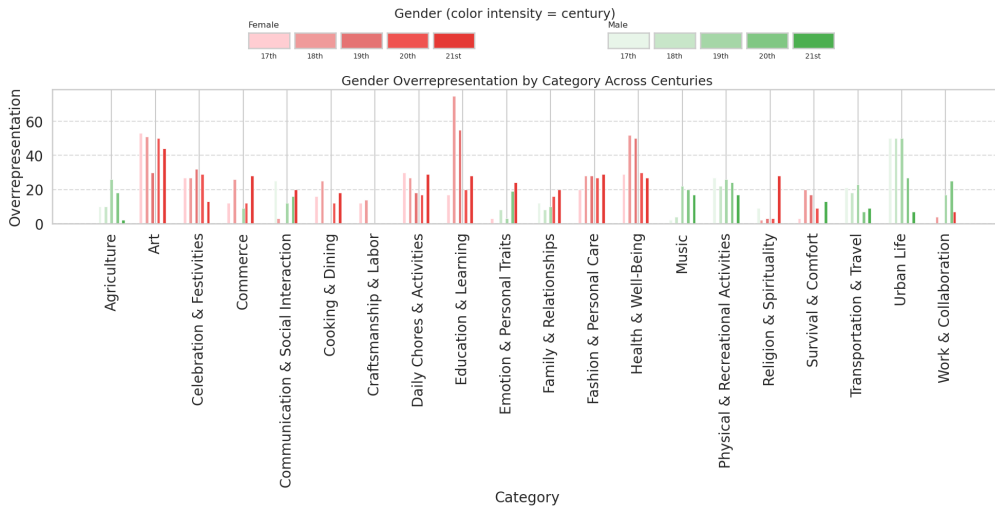


Figure 23: Over- and underrepresentation of gender predictions across **centuries** for **SD3**.

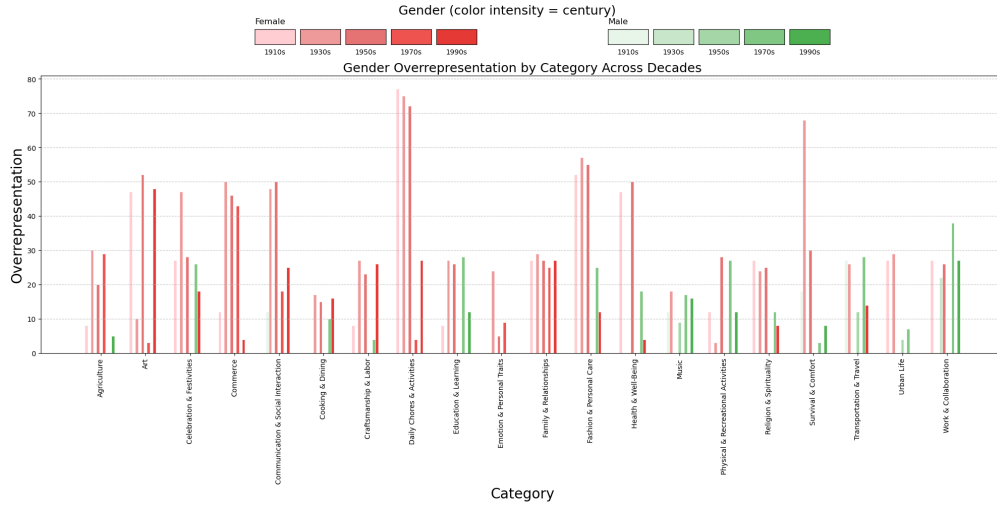


Figure 24: Over- and underrepresentation of gender predictions across **decades** for **SD3**.

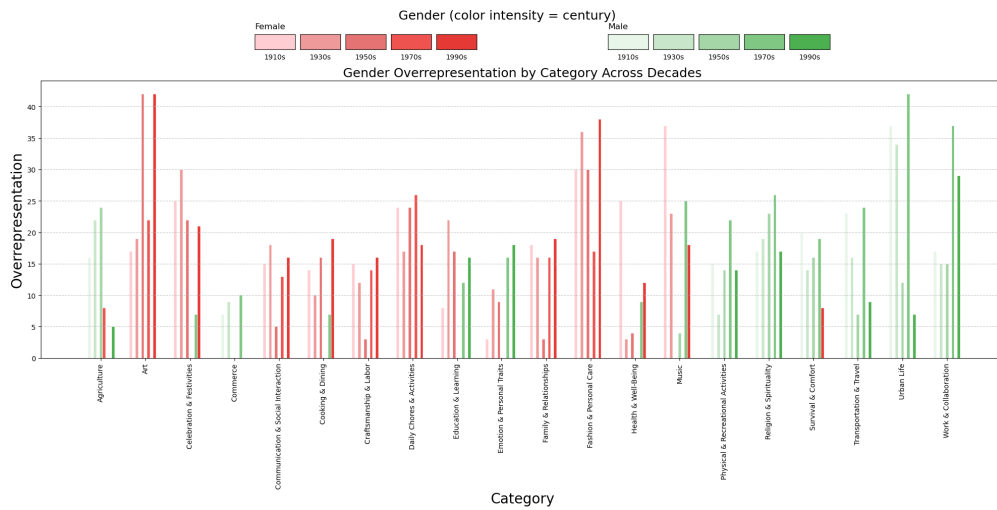


Figure 25: Over- and underrepresentation of gender predictions across **decades** for **SDXL**.

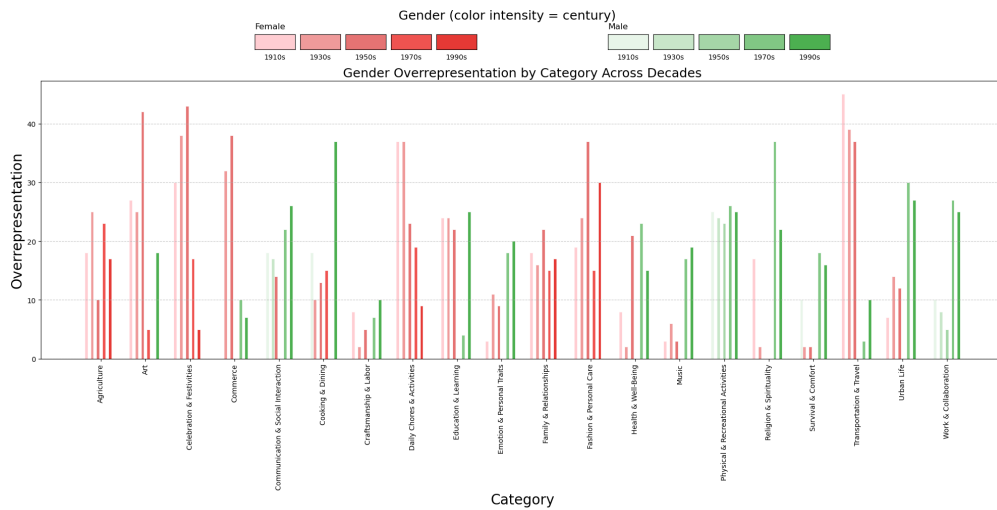


Figure 26: Over- and underrepresentation of gender predictions across **decades** for **FLUX.1**.

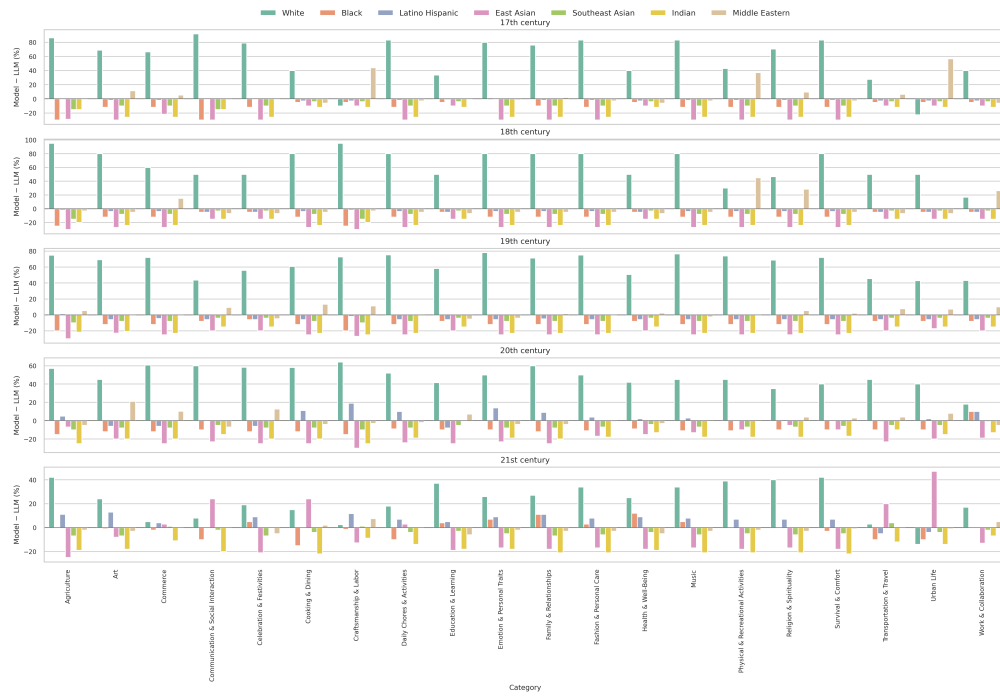


Figure 27: Racial over- and underrepresentation across centuries for **FLUX.1**.

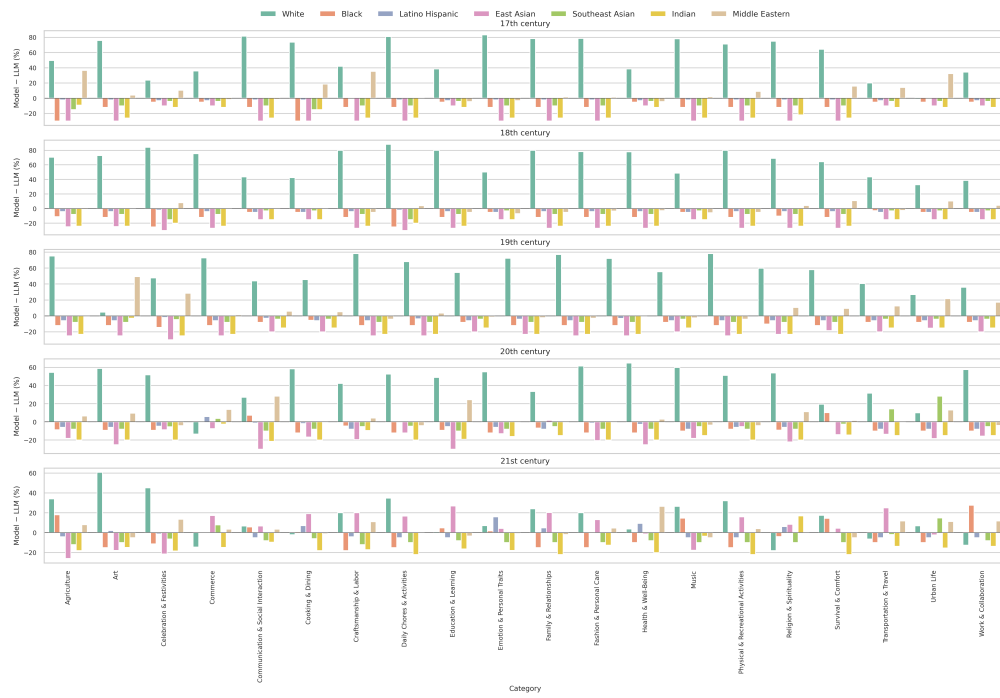


Figure 28: Racial over- and underrepresentation across centuries for **SD3**.

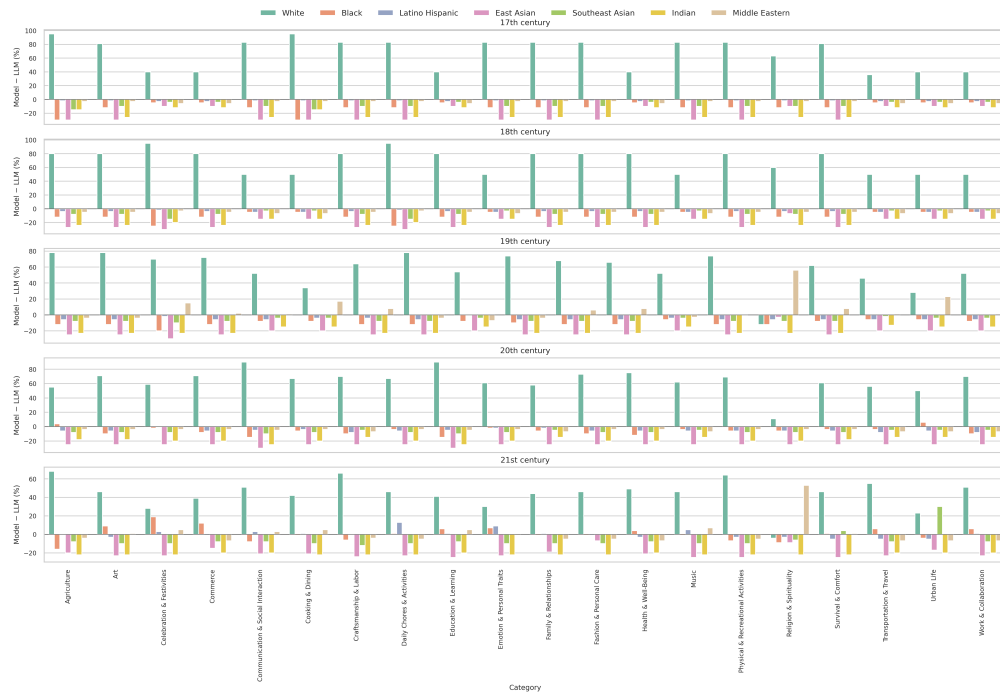


Figure 29: Racial over- and underrepresentation across centuries for **SDXL**.

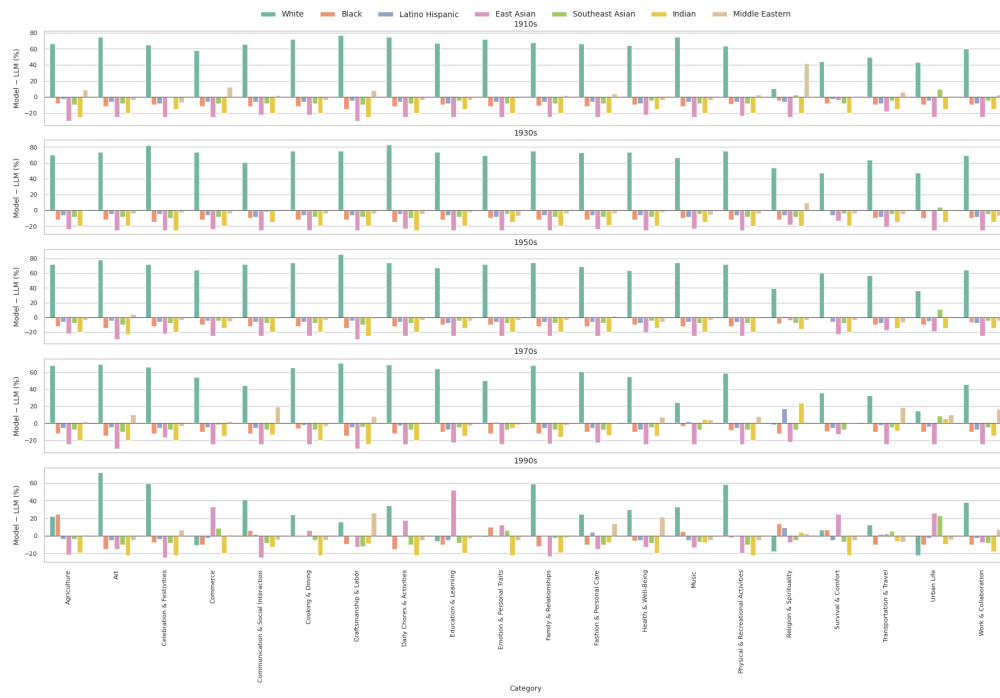


Figure 30: Racial over- and underrepresentation across decades for **SD3**.

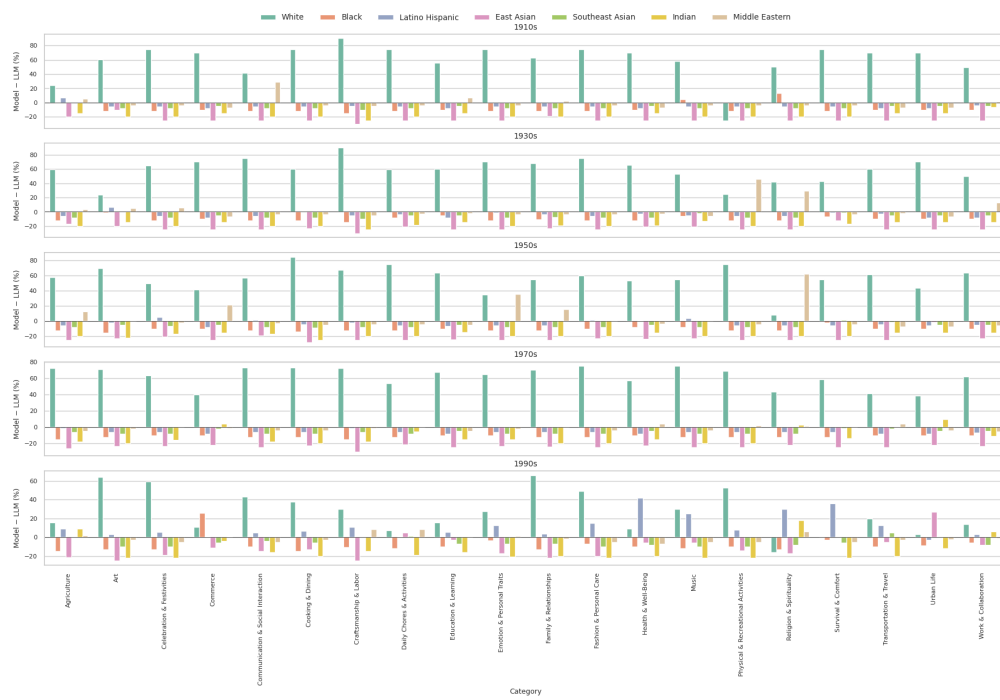


Figure 31: Racial over- and underrepresentation across decades for **FLUX.1**.